# "EVALUATION OF RING ENHANCING LESIONS IN BRAIN IN CORRELATION WITH ARTERIAL SPIN LABELING AND MR SPECTROSCOPY"

**By**

**REG NO: BS0120006**

# Dissertation

**Submitted to the**
**KLE Academy of Higher Education and Research,**
**Belagavi, Karnataka**
**In partial fulfillment**
**of the requirements for the degree of**

**M.D.**
**IN**
**RADIO-DIAGNOSIS**

**DEPARTMENT OF RADIO-DIAGNOSIS,**

**J. N. MEDICAL COLLEGE,**

**BELAGAVI -590010. KARNATAKA**

**JUNE / JULY 2023**

**KLE Academy of Higher Education and Research,**
**Belagavi, Karnataka**

# ENDORSEMENT

This is to certify that the dissertation entitled **"EVALATION OF RING ENHANCING LESIONS IN BRAIN IN CORRELATION WITH ARTERIAL SPIN LABELING AND MR SPECTROSCOPY"** is a bonafide research work done by **REG NO. BS0120006.**


**Dr. PRADEEPGOUD PATIL** MD
Professor & Head
Department of Radiodiagnosis
J.N. Medical College,
Nehru Nagar,
Belagavi- 590010

**Date:** 18/01/2023
**Place: Belagavi**

**Dr. N. S. MAHANTSHETTI** MD
Principal
J.N. Medical College
Nehru Nagar,
Belagavi- 590010

**Date:**
**Place: Belagavi**

# UNDERTAKING

I **REG NO. BS0120006,** hereby declare that the information and the data mentioned in my dissertation entitled **"EVALATION OF RING ENHANCING LESIONS IN BRAIN IN CORRELATION WITH ARTERIAL SPIN LABELING AND MR SPECTROSCOPY"** belongs to me and is original. I am aware of the definition of plagiarism as detailed below:

- An act or instance of using or closely imitating the language and thoughts of another author without authorization and the representation of that author's work as one's own, as by not crediting the original author.
- A piece of writing or other work reflecting such unauthorized use or imitation.
- The deliberate or reckless representation of another's words, thoughts or ideas as one's own without attribution in connection with submission of academic work, whether graded or otherwise.

I hereby declare that the dissertation prepared by me is original one and does not involve plagiarism anywhere. In case at a later stage, it is found that I have indulged in plagiarism, then I am solely responsible for the same and the institution is at liberty to take any disciplinary action against me including cancellation of dissertation or any other penalties imposed by the University.

Date: 18/01/23
Place: Belagavi

**REG NO. BS0120006**

# PLAGIARISM CERTIFICATE

KLE ACADEMY OF HIGHER EDUCATION AND RESEARCH

**JAWAHARLAL NEHRU MEDICAL COLLEGE**

(Recognized by Medical Council of India, New Delhi)

**Accredited 'A+' Grade by NAAC (3rd Cycle)** **Placed in Category 'A' by MHRD (GoI)**

*Nehru Nagar, Belagavi- 590 010, Karnataka, INDIA*

0831 - 2471350 0831 - 2470759 www.jnmc.edu principal@jnmc.edu

Ref No: MDC/PG/ Date: 26-12-2022.

## ACCEPTANCE LETTER

The softcopy of thesis entitled: **"EVALUATION OF RING ENHANCING LESIONS IN BRAIN IN CORRELATION WITH ARTERIAL SPIN LABELING AND MR SPECTROSCOPY"** has been submitted for Anti-Plagiarism check through Turnitin software. The scan has been carried out and the scanned output reveals a match percentage of **06%** which is within the acceptable limits of **10%** as per the guidelines given by UGC.

**Guide.**

KAHER BELAGAVI J. N. MEDICAL COLLEGE

**Dr. (Mrs.) N.S. Mahantashetti.**
Chairperson-Antiplagiarism Committee &
Principal,
J. N. Medical College, Belagavi.

To,
**Reg. No. BS0120006**
Postgraduate Student,
2020-21 Batch,
Department of Radiology,
J. N. Medical College, Belagavi.

# ETHICAL CLEARANCE LETTER

K.L.E. ACADEMY OF HIGHER EDUCATION AND RESEARCH
(Deemed – to- be- University)
Accredited 'A' Grade by NAAC (2nd Cycle) Placed in Category 'A' by MHRD (GoI)
**JAWAHARLAL NEHRU MEDICAL COLLEGE,**
**NEHRU NAGAR, BELAGAVI-590010 (KARNATAKA-INDIA)**
Website: http//www.jnmc.edu
E-Mail : dome@jnmc.edu
Phone: (+91-(0)831 Office : 2472550
Principal: 2471701
Fax No. +91 (0)831 – 2470759

**Ref: MDC/DOME/** 144 **Date: 25/01/2021**

To,

PG student in Radio-diagnosis,
J.N.Medical College,
BELAGAVI.

Sub: Institutional Ethical Clearance for the study.

With reference to the above, we wish to inform you that your proposed research project titled **"EVALUATION OF RING ENHANCING LESIONS IN BRAIN IN CORRELATION WITH ARTERIAL SPIN LABELING AND MR SPECTROSCOPY"**, is ethical and justifiable. The proposed research project has been cleared by the JNMC Institutional Ethics Committee on Human Subjects Research.

**(Dr. Smita Sonoli)**
Member Secretary
JNMC Institutional Ethics Committee
on Human Subjects Research,
J.N.Medical College, Belagavi.

**(Dr. Harsha Hegde)**
Chairman,
JNMC Institutional Ethics Committee
on Human Subjects Research,
J.N.Medical College, Belagavi.

# ABBREVIATIONS

| | | |
|---|---|---|
| ASL | - | Arterial spin labelling |
| CBF | - | Cerebral blood flow |
| CBV | - | Cerebral blood volume |
| Cho | - | Cholines |
| CN | - | Central nervous system |
| Cr | - | Creatine |
| CT | - | Computerized topography |
| GABA | - | γ-Amino-butyric acid |
| Glu | - | Glutamate |
| MRI | - | Magnetic resonance imaging |
| MRS | - | Magnetic resonance spectroscopy |
| NAA | - | N acetyl aspartate |
| NAAG | - | N-Acetylaspartylglutamate |
| NCC | - | Neurocysticercosis |

# ABSTRACT

**BACKGROUND:** Ring enhancing intracranial lesions are common and are considered as a diagnostic dilemma. Although MRI has been established as the most reliable diagnostic methods, it had limited role in quantitative and functional assessment. ASL and MRS can also help in differentiating the high-grade forms from low grade tumours. Further classify ring enhancing lesions, will help in better diagnosis, classification, grading and treatment. Hence, the present study was conducted to analyse ring enhanced lesions on MR scan by using such advanced diagnostic techniques and classify the tumours.

**METHODOLOGY:** Cross-sectional observational study for a period of one year by including 35 patients detected with single or multiple ring enhancing lesions of MRI Brain Scan, who are referred to Radiodiagnosis for ASL perfusion and MR Spectroscopy.

**RESULTS:** Average age of our patients was 63.8±9.4 years. There was no significant correlation observed between the demographic details and the incidence of lesions either on MRS or on ASL. Headache in 60% study samples was the common symptoms. Hypodense lesions were higher with the proportion of 48.6% (17) on T1 morphology. 82.9% (29) patients hyperdense in T2. Diffusion was restricted among 71.4% patients. Choline and NAA peak were the most common finding observed with the incidence of 7 (20%), followed by lipid lactate among 6 (17.1%) of the patients included in our study. 8 (22.9%) each of the patients were diagnosed with tuberculoma and high-grade Glioma were the most common findings. Cerebral flow was significantly higher among the neoplastic lesions compared to non-neoplastic and

significantly greater among primary neoplastic lesions than the metastatic lesions. Average nCBFL and nCBFPE were significantly higher among neoplastic lesions than non- neoplastic lesions.

**CONCLUSION:** Multiple ring enhancing lesions are seen on MRI brain and contrast studies which can suggestive multiple diagnosis in lacing neoplastic aetiologies as well as being aetiologies. Hence ASL is one of the reliable diagnostic tools for differentiating neoplastic and non-neoplastic lesions, and from differentiating neoplastic primary lesions from metastasis. Further added MR spectroscopy helps in conformation of the diagnosis. A combination of the 3 help in getting closer to the accurate diagnosis thereby reducing the need off biopsies, helping to start early treatment.

**KEY WORDS:** Ring enhancing lesions, MRS, MRI, ASL

# TABLE OF CONTENTS


| SL.NO | CONTENT | PAGE NO. |
|---|---|---|
| 01 | INTRODUCTION | 1-2 |
| 02 | AIMS AND OBJECTIVE | 3 |
| 03 | REVIEW OF LITERATURE | 4-41 |
| 04 | MATERIALS AND METHODS | 42-45 |
| 05 | RESULTS AND STATISTICAL ANALYSIS | 46-58 |
| 06 | DISCUSSION | 59-70 |
| 07 | CONCLUSION | 71 |
| 08 | SUMMARY | 72-73 |
| 09 | BIBLIOGRAPHY | 74-83 |
| 10 | ANNEXURES | 84-88 |
| | Annexure I – Consent | 84-87 |
| | Annexure II – Proforma | 88 |
| | Annexure III – Master Chart | |

# LIST OF TABLES


| TABLE NO. | DESCRIPTION | PAGE NO. |
|---|---|---|
| **1.** | Pattern of Distribution of age | **46** |
| **2.** | Pattern of Distribution of gender | **48** |
| **3.** | Pattern of distribution of symptoms | **49** |
| **4.** | Pattern of distribution of T1 morphology | **50** |
| **5.** | Pattern of distribution of T2 morphology | **51** |
| **6.** | Pattern of distribution of diffusion restriction | **52** |
| **7.** | Distribution of spectroscopy | **53** |
| **8.** | Distribution of diagnosis | **55** |
| **9.** | Mean values of nCBFL and nCBFPE in various lesions | **57** |
| **10.** | Mean nCBFL and nCBFPE values among neoplastic and non- neoplastic group | **58** |

# LIST OF FIGURES AND GRAPHS


| TABLE NO. | DESCRIPTION | PAGE NO. |
|---|---|---|
| **1.** | H1MRS spectra: Anerobic metabolism | **19** |
| **2.** | H1MRS spectra: Lymphoma | **20** |
| **3.** | H1MRS spectra: Tumor recurrence | **21** |
| **4.** | Physiological hyper-perfusion in bilateral occipital cortex | **26** |
| **5.** | Statistical parametric map of significant cerebral blood flow differences between Alzheimer's and control patients. | **27** |
| **6.** | ASL illustrating cerebral blood flow from a patient by Zaharchuk G et al | **28** |
| **7.** | Soft tissue vascular anomaly found in 13-month-old child | **30** |
| **8.** | Representative images from two patients with AD comparing with ASL | **31** |
| **9.** | Magnetic resonance imaging of 11-year-old male child for seizure evaluation | **33** |
| **10.** | T2W1 of A case of abscess in the left frontoparietal lobe | **35** |
| **GRAPH NO.** | **GRAPHS** | **PAGE NO** |
| **11.** | Pattern of Distribution of age | **47** |
| **12.** | Pattern of Distribution of gender | **48** |
| **13.** | Pattern of distribution of symptoms | **49** |
| **14.** | Pattern of distribution of T1 morphology | **50** |

| | | |
|---|---|---|
| **15.** | Pattern of distribution of T2 morphology | **51** |
| **16.** | Pattern of distribution of diffusion restriction | **52** |
| **17.** | Distribution of spectroscopy | **54** |
| **18.** | Distribution of diagnosis | **56** |
| **19.** | Mean values of nCBFL and nCBFPE in various lesions | **57** |
| **20.** | Mean nCBFL and nCBFPE values among neoplastic and non-neoplastic group | **58** |

# INTRODUCTION

Ring enhancing intracranial lesions are common and are considered as a diagnostic dilemma. This A ring-enhancing lesion in brain imaging is also a common feature on the Indian subcontinent. These lesions might present as a solitary or multiple on a brain MRI and are characterised by a contrast enhancing halo with a non-enhancing centre. [1]

It is difficult to distinguish neoplastic lesions such as gliomas, lymphoma or metastasis from non-neoplastic lesions like tuberculosis, neurocysticercosis, fungal infections, demyelinating lesions, sarcoidosis, Bechet disease, radiation encephalopathy and other vascular causes on conventional MRI. [2,3]

Although MRI has been established as the most reliable diagnostic methods, it had limited role in quantitative and functional assessment of lesions thus making it less reliable in differentiating the tumour like lesions. As the size, shape, wall thickness of ring-enhancing lesions, the extent of surrounding edema has to be considered in analysing the lesions, advanced imaging techniques gives the better imaging than the conventional methods.[2]

Hence, the advanced MR techniques are required to study such lesions further. Arterial spin labelling is one such advanced, non-invasive methods that provides absolute quantification of cerebral blood flow in the absence of contrast that helps in estimating tumour neo-genesis which in turn helps in tumour grading, biopsy and surgical planning. [3,4]

MR spectroscopy is another methos used for the evaluation of brain tumours, that detects tumour metabolism. Almost all brain tumours have decreased N-acetyl aspartate (NAA) signals and increased levels of Choline (Cho) which causes increase in Cho/NAA ratio.[5,6]

Other common metabolic changes like increase in lactate levels due to anaerobic glycolysis or increase in lipid levels due to necrosis can be detected on MR spectroscopy which helps in the diagnosis of tumours and other causes.[7]

ASL and MRS can also help in differentiating the high-grade forms from low grade tumours. As these techniques can further classify ring enhancing lesions, this study will help in better diagnosis, classification, grading and treatment, which will be helping in the overall patient care and diagnosis. Hence, the present study was conducted to analyse ring enhanced lesions on MR scan by using such advanced diagnostic techniques and classify the tumours.

# AIM AND OBJECTIVES

- To detect Ring enhancing lesions on MRI Scan and further use advanced MR techniques like Arterial Spin labeling (ASL) and MR Spectroscopy to differentiate them into Benign and Malignant lesions (High grade versus low grade, primary versus metastatic)
- To further characterize these rings enhancing lesion into neuro infections, abscess, demyelinating lesions and other lesions.

# REVIEW OF LITERATURE

## HISTORICAL DEVELOPMENTS IN MRI

The nuclear magnetic resonance (NMR) phenomenon was first described experimentally by both Bloch and Purcell in 1946, for which they were both awarded the Nobel Prize for Physics in 1952.

The technique has rapidly evolved since then, following the introduction of wide-bore superconducting magnets, approximately 30 years ago, allowing development of clinical applications. The first clinical magnetic resonance images were produced in Nottingham and Aberdeen in 1980, and magnetic resonance imaging (MRI) is now a widely available, powerful clinical tool.[9]

## BRIEF INTRODUCTION ABOUT MRI

Magnetic resonance imaging (MRI) uses the body's natural magnetic properties to produce detailed images from any part of the body. For imaging purposes, the hydrogen nucleus which has a single proton is used because of its abundance in water and fat.[10,11]

MRI scanners come in different field strengths, usually between 0.5 and 1.5 tesla. Different tissues such as fat and water have different relaxation times and can be identified separately. By using a “fat suppression” pulse sequence, for example, the signal from fat will be removed, leaving only the signal from any abnormalities lying within it.[12]

## RING ENHANCING LESIONS ON MRI

Cerebral ring-enhancing lesions are defined as an area of hypodensity in computed tomography or hypo-intensity in magnetic resonance imaging [MRI] of the brain tissue surrounded by a rim of enhancing tissue after contrast injection.

Presentation of diseases varies depending on the site, extent of brain involvement and the etiology. It is always important to correlate clinical symptoms and any previous imaging as the same imaging appearance can suggest vastly different etiologies with variation in disease presentation. [13]

Differential for peripheral or **ring enhancing cerebral lesions** includes:

- Cerebral abscess
- Tuberculoma
- Neurocysticercosis
- Metastasis
- Glioblastoma
- Subacute infarct/haemorrhage/contusion
- Demyelination (incomplete ring)
- Tumefactive demyelinating lesion (incomplete ring)
- Radiation necrosis
- Postoperative change
- Lymphoma - in an immunocompromised patient
- Leukemia
- Thrombosed aneurysm
- Necrotizing leukoencephalopathy after methotrexate
- Baló concentric sclerosis

No single feature is pathognomonic, although a cystic lesion that markedly restricts centrally on DWI should be considered an abscess until proven otherwise.

Many features of the lesion, as well as clinical presentation and patient demographics, need to be taken together to help narrow the differential. Helpful rules of thumb include:

**Enhancing wall characteristics as in;**

- Thick and nodular which favours neoplasm
- Thin and regular favouring the abscess
- Incomplete ring often opened toward the cortex favours demyelination
- Intermediate to low T2 signal capsule indicating the abscess
- Restricted diffusion of enhancing wall favours GBM or demyelination

**Surrounding oedema**

- Extensive oedema relative to lesion size which will be depicting abscess
- Increased perfusion favours neoplasm or metastases or primary cerebral malignancy.

**Central fluid content:**

- Restricted diffusion favours abscess
- An absence of diffusion restriction favours a tumour with a central necrotic component which is the classic features of metastases.

**Number of lesions:** Similar sized rounded lesions at grey-white matter junction favours metastases or abscesses irregular mass with adjacent secondary lesions

embedded in the same region of 'oedema' favours GBM. small (<1-2 cm) lesions with thin walls, especially if other calcific foci are present, suggest neurocysticercosis.[14,15]

**Differential diagnosis of the various lesion in brain on MRI**[16]

**Tuberculoma:** Tuberculoma is granulation tissue that occurs following central nervous system (CNS) tuberculosis infection. It differs to the much less common tuberculosis abscess that is a true collection of pus. It can occur with or without tuberculous meningitis.

The lesion is usually T1 hypointense and T2 hypointense/isointense. However, T2 hyperintensity may be noted when there is central liquified caseating material.

Enhancement pattern is usually ring-shaped but a mass like enhancing pattern may sometimes be seen. The presence of concomitant basal cistern leptomeningeal enhancement suggests meningitis with a high probability of CNS tuberculosis as the underlying aetiology.[1]

**Fungal Abscess**: Rare cause of cerebral ring-enhancing lesion. It usually occurs in immunocompromised individuals such as those prescribed immunosuppressive therapies or having undergone organ transplantation. On MRI, the lesions are usually T1 hypointense and T2 hyperintense with no suppression on FLAIR sequence. Pyogenic abscesses are likely to be solitary and rarely involve the basal ganglia. Characteristic feature in fungal abscess is restricted diffusion of the abscess. In pyogenic abscess, the cavity shows marked restricted diffusion.[1,16]

**Cerebral Toxoplasmosis**: Parasitic infection in the brain with Toxoplasma gondii. The lesion appears T1 hypointense and T2 hyperintense. The abscess wall appears T2 hypointense. In immunocompetent, infection is often asymptomatic. On MRI,

cerebral toxoplasmosis usually appears as multiple small abscesses at the grey-white junction, basal ganglia, and thalami. They are usually T1 isointense to hypointense with variable T2 signal. No definite restricted diffusion within the abscess cavity is seen. Ring enhancement is often seen on contrast injection. The characteristic "eccentric target sign" is highly specific for cerebral toxoplasmosis but is only present in 30% of cases. The lesion has an inner eccentric enhancing core surrounded by a hypointense zone and an outer peripherally enhancing rim, overall giving an eccentric mural nodule appearance.

**Neurocysticercosis**: Caused by CNS infection with the pork tapeworm Taenia solium. The disease is endemic in certain parts of Asia, Africa, and America. The most common presentation in endemic areas is seizure. Other presentations will depend on the site of involvement in the brain. Neurocysticercosis develops over four stages.

Vesicular stage: The membrane of the parasite is intact and the parasite is viable.

Colloidal vesicular stage: The parasite dies and the membrane becomes leaky. Significant adjacent oedema around different parasitic lesions.

Granular nodular stage: Extent of oedema decreases.

Nodular calcified stage: Calcified with no more adjacent oedema.

MRI features of neurocysticercosis are essentially thin-walled ring-enhancing lesions. The lesions can be distributed at the subarachnoid space, brain parenchyma especially grey-white junction, and the ventricles of the brain. At the early stage, enhancing nodules may be seen within the ring-enhancing lesions. However, the most typical appearance of neurocysticercosis is multiple calcified nodules with no

significant oedema in the final nodular calcified stage. Hypointensity is seen on T2-weighted sequence due to underlying calcification. Differing from dystrophic calcification of brain, persistent ring enhancement can be noted despite calcification of the lesion

**Glioblastoma**: High-grade astrocytoma and is the most common primary brain tumour in adults. It can be classified as primary or secondary: arising from a low-grade astrocytoma. Most primary glioblastomas are isocitrate dehydrogenase wild-type whereas secondary glioblastoma is more likely to have isocitrate dehydrogenase–mutant status.

Up to 90% of glioblastomas are primary and more commonly seen in elderly patients. The tumour arises in cerebral white matter and has a high tendency to spread across the corpus callosum. Similar to most brain tumours, it is T1 hypointense and T2 hyperintense, but the irregular ring enhancement is a feature of glioblastoma, often associated with a thick enhancing rim. Prognosis of the disease is generally very poor due to its fast growth and aggressive behaviour.

**Brain Metastasis**: More common intracranial malignancy than primary malignant brain tumour. Common tumours that metastasise to the brain include those of lung cancer, malignant melanoma, renal cell carcinoma, breast cancer, and colorectal carcinoma.13 Brain metastasis can be solitary or multiple.

Most metastatic lesions are T1 hypointense and T2 hyperintense except for malignant melanoma, in which the intrinsic melanin pigment will cause a reduction in T1 relaxation time with a consequent T1 hyperintense appearance. When the tumour is complicated with haemorrhage, T1 hyperintensity of the lesion will be noted.

Enhancement can be uniform or ring-shaped and the wall of ring-enhancing lesions is often thick and irregular.

Differentiation between metastases and primary glioblastoma may be difficult because the latter may also present with multiple enhancing foci. For metastases, they tend to involve the grey-white junction and rarely spread along the corpus callosum unlike those of glioblastoma.

Moreover, if multiple enhancing tumours are not connected by a single patch of T2/FLAIR abnormality, they are more likely due to metastases. If the same characteristic is seen in glioblastoma, it is termed multicentric glioblastoma and considered a rare entity since it means there are multiple synchronous glioblastoma within the brain.

**MR spectroscopy** may be useful to **distinguish the two diseases** by investigation of the region of T2 hyperintensity around the ring of enhancement. In metastases, the region of adjacent T2 hyperintensity often represents vasogenic oedema and there will not be any increased choline-to-creatinine ratio. In glioblastoma, the T2 hyperintensity might represent non-enhancing tumour infiltration and will be evidenced by increased choline-to-creatinine ratio at those region

**Primary Central Nervous System Lymphoma**: No systemic lymphomatous involvement when the disease is diagnosed. Otherwise, it is just classified as secondary intracranial involvement of lymphoma.

The presentation again depends on the location and size of the lesions. One special characteristic of primary CNS lymphoma is a predilection for supratentorial white matter. Similar to glioblastoma, it has a tendency to spread across the corpus callosum.

On CT, it appears as a homogenous hyperdense lesion with diffuse contrast enhancement. On MRI, primary CNS lymphoma is typically T1 hypointense and T2 hypointense/isointense with restricted diffusion.

The T2 hypointensity of primary CNS lymphoma makes it a special characteristic as most intracranial masses are T2 hyperintense. In immunocompetent patients, primary CNS lymphoma usually demonstrates homogenous enhancement with diffuse restricted diffusion. In immunocompromised patients, the enhancement pattern is more heterogeneous and the lesion will more likely demonstrate ring enhancement. Central necrosis of tumour tends to occur in immunocompromised patients, so focal T2 hyperintensity may be evident within the lesions. A characteristic of MR spectroscopy in primary CNS lymphoma is markedly elevated cholineto-creatinine ratio.

**POST-RADIATION CAUSE**: Pseudo-progression and Cerebral Radiation Necrosis Brain tumours such as glioblastoma and brain metastases often require radiation therapy. This often imposes diagnostic challenges as post-radiation changes to the tumour may simulate the appearance of residual or recurrent tumour. Pseudo-progression and cerebral radiation necrosis are both sequelae of radiation

Occurs in the first 3 months following completion of brain radiation but can occur up to 6 months post-treatment. It appears as an enlarging irregular ring-enhancing lesion mimicking disease progression whereas it actually represents a change related to underlying cell death. The border of the lesion with pseudo progression might have a “Swiss cheese” or “soap bubble” appearance.

A few advanced MR sequences may contribute to diagnosis of pseudo progression. On MR perfusion scan, pseudo progression will show reduced cerebral blood volume whereas tumour usually has increased cerebral blood volume. MR spectroscopy of pseudo progression often shows reduced metabolites and increased lactate peak. Stability or shrinkage of the lesion through interval follow-up imaging can also confirm that the lesion is related to post-radiation changes.

Cerebral radiation necrosis refers to a more long-term effect of radiation therapy, usually beyond 6 months to years after treatment. The mass effect of the lesion will be lost, unlike pseudo progression. On the other hand, the enhancing features, and findings on MR spectroscopy and MR perfusion are similar to those of pseudo progression.

**EMYELINATING CAUSE**: Multiple Sclerosis One of the most common demyelinating diseases is multiple sclerosis. The disease has several presentation patterns. Involvement can be at the cerebrum, cerebellum, brain stem, cranial nerves especially optic nerves, and spinal cord.

In general, multiple sclerosis is predominantly seen in women, with a female-to-male ratio up to 2:1.21 MRI is the important imaging modality in the radiological diagnosis of multiple sclerosis. Diseased regions typically show foci of T1 hypointensity and T2/FLAIR hyperintensity, with a predilection for the callososeptal interface. They can slowly progress with longitudinal extension perpendicular to the lateral ventricles, giving the typical “Dawson’s fingers” appearance.

Post-contrast and DWI sequences are useful to detect active lesions/plaque. Sometimes these active lesions may be quite large and mimic a mass lesion. Active demyelinating lesions can be distinguished from other malignant causes by the special

ring-enhancing pattern seen in the demyelinating disease known as "open ring enhancement",22 which means there is incomplete ring enhancement. The enhancing edge represents an active demyelinating process in those regions. This sign is rather specific for demyelination as the underlying cause.

**VASCULAR CAUSE**: Haematoma Hypertensive intracranial haemorrhage is the most common cause of intracranial haemorrhage. It typically affects the basal ganglia, thalami, cerebellum, and pons. When the haematoma enters a subacute phase or early chronic phase, thin peripheral enhancement around the haematoma is often evident and may mimic tumour mass lesion. Imaging characteristics of subacute haematoma include T1 and T2 hyperintensity of the lesion.

Also, the peripheral ring enhancement should be thin. Perilesional vasogenic oedema is usually not very significant. A haemosiderin rim that is complete is often seen on T2- weighted image and blooming artefact is noted on DWI sequence. Interval follow-up scan can exclude malignant lesions that will progress in size. If MR perfusion is available, the cerebral blood flow will decrease in case of subacute haematoma.[1,14-16]

**Magnetic resonance spectroscopy**

In vivo magnetic resonance spectroscopy (MRS) of the human brain has developed rapidly since its first observation in the 1980s.[17]

- Early studies in both humans and animals focused on the $^{31}P$ nucleus which allowed the measurement of energy metabolites such as phosphocreatine and ATP, as well as inorganic phosphate and phosphoesters.
- With the development of improved techniques for spatial localization and water suppression, proton MRS became more prevalent in the 1990s because of its

higher sensitivity and greater convenience as it can be performed without hardware modification on most MRI machines, unlike MRS of other nuclei. [17,18]

## BASIC PRINCIPLE OF MRS

The identification of different chemicals in a tissue is based on the fact that protons in different molecules with different atomic numbers process at different frequencies.

This difference in frequencies are derived from the populace of electron cloud surrounding the protons. As electrons are charged particles, they show magnetic spin properties and when exposed to external magnetic field (B0) generates a small magnetic field (B*). [19]

As a result, magnetic environment surrounding the nucleus and hence protons are modified minimally expressed in parts per million of the external magnetic field (B0).

Consequently, the resonance frequency of the nucleus, which is directly proportional to the magnetic field it experiences, shifts. This phenomenon is known as chemical shift and forms the basis of MR spectroscopy.[17,18]

## COMPOUNDS DETECTED BY MRS[20]

1. **N acetyl aspartate (NAA):** NAA is the largest signal in the normal adult brain spectrum. NAA is one of the most abundant amino acids in the central nervous system. It has been speculated to be a source of acetyl groups for lipid synthesis, a regulator of protein synthesis, a storage form of acetyl-CoA or aspartate, a breakdown product of NAAG or an osmolyte. NAA does appear to be a

good *surrogate* marker of neuronal health but it might sometimes change independent of neuron cell density or function. Central neurocytoma, an uncommon neuronal tumor, have been reported to exhibit detectable NAA peak, although with decreased NAA/Cr. [20,21]

2. **Choline (Cho):** The "choline" signal ("Cho," 3.20 ppm) is a composite peak consisting of contributions from the trimethylamine groups of glycerophosphocholine (GPC), phosphocholine (PC) and a small amount of free choline itself. In pathological demyelination, we can observe elevated choline or even due to inflammatory conditions of the brain. Low brain Cho has been observed in hepatic encephalopathy and there is also some evidence to suggest that dietary intake of choline can modulate cerebral Cho levels.[20,22]

3. **Lactate:** The lactate resonance is usually not detectable in the brain under normal conditions. However, lactate is often detected by MRS in pathological conditions such as acute hypoxic or ischemic injury or in brain tumours or mitochondrial diseases. Also, it produces doublet peak.[20,23]

4. **Alanine:** Alanine peak is produced by transamination of pyruvate in hypoxic tissues showing increased glycolysis to prevent further increase in lactate. Amongst the brain tumors, meningiomas show a distinct alanine peak with variable sensitivity. Alanine in meningiomas has been postulated to be a partial oxidation of glutamine. Alanine peak is also elevated in central neurocytoma and PNET. [24]

5. **Acetate and succinate:** Raised acetate and succinate levels reflect anaerobic fermentation of pyruvate generated from glycolysis where it undergoes carboxylation to form acetate and succinate. Although these peaks might be

slightly raised in brain tumors, clinically the presence of markedly raised acetate and succinate peaks in the MR spectra is useful for identifying brain abscesses that mimic brain tumors on conventional MR. [25]

6. **Myo-inositol:** Glial cells in vitro have been shown to contain higher levels of mI than neurons, reduced in hepatic encephalopathy, increased in Alzheimer's dementia and other demyelinating disorders. [26]

7. **Creatine:** In the clinical MR spectroscopy Cr peak is utilized as internal reference standard for characterizing other peaks as its level is high and relatively comparable in different tissue types of brain. Glial tumours show 15–40% reduction in Cr levels. Even meningotheliomatous meningiomas which shows approximately 20% reduction in total creatine. Total creatine content is significantly low in non-neuroectodermal tumors such as brain metastases compared to neuroectodermal tumors. [18,20,27]

8. **Glutamate:** Most abundant and dominant neuro-transmitter. Elevated in MS plaques.[20]

9. **Membrane lipids:** Rise of lipids detected in various cellular processes such as necrosis, growth arrest, inflammation, malignancy and apoptosis. Membrane lipids are usually not recognized on standard MRS unless imaged at very short echo time.[28]

10. **Taurine:** Taurine shows two triplet peaks. It is an inhibitory neurotransmitter that activates GABA-A receptors or strychnine-sensitive glycine receptors. Increased taurine is seen in PNET, medulloblastoma, pituitary microadenoma and metastatic renal cell carcinoma. High levels in medulloblastoma points

towards morphogenetic similarities between medulloblastoma and retinoblastomas as retina contains one of the highest levels of taurine owing to the presence of its high affinity transport system.[18,20,29]

11. **Other uncommon components:** All the common and uncommon components found on MRS are tabulated below.[20]

**Table 1: Compounds detected by MRS in the human brain[20]**

| **Compounds normally present** | **Compounds which may be detected under pathological or other abnormal conditions** |
|---|---|
| ***Large signals at long TE*** | ***Long TE*** |
| *N*-Acetylaspartate (NAA) | Lactate (Lac) |
| Creatine (Cr) and phosphocreatine (PCr) | β-Hydroxy-butyrate, acetone |
| Cholines (Cho): | Succinate, pyruvate |
| Glycerophosphocholine (GPC) | Alanine |
| Phosphocholine (PC), free choline (Cho) | Glycine |
| ***Large signals at short TE*** | ***Short TE*** |
| Glutamate (Glu) | Lipids |
| Glutamine (Gln) | Macromolecules |
| *myo*-Inositol (mI) | Phenylalanine |
| | Galactitol |
| ***Small signals (short or long TE)*** | ***Exogenous compounds (short or long*** |
| *N*-Acetylaspartylglutamate (NAAG), aspartate | Propan-1,2-diol Mannitol |
| Taurine, betaine, *scyllo*inositol, ethanolamine | Ethanol Methyl sulfonyl methane (MSM) |
| Threonine | |

| | |
|---|---|
| Glucose, glycogen | |
| Purine nucleotides | |
| Histidine | |
| ***Small signals that can be detected with the use of spectral editing techniques*** | |
| γ-Amino-butyric acid (GABA) | |
| Homocarnosine | |
| Glutathione | |
| Threonine | |
| Vitamin C (ascorbic acid) | |

**Few evidences of spectra of various brain tumours**

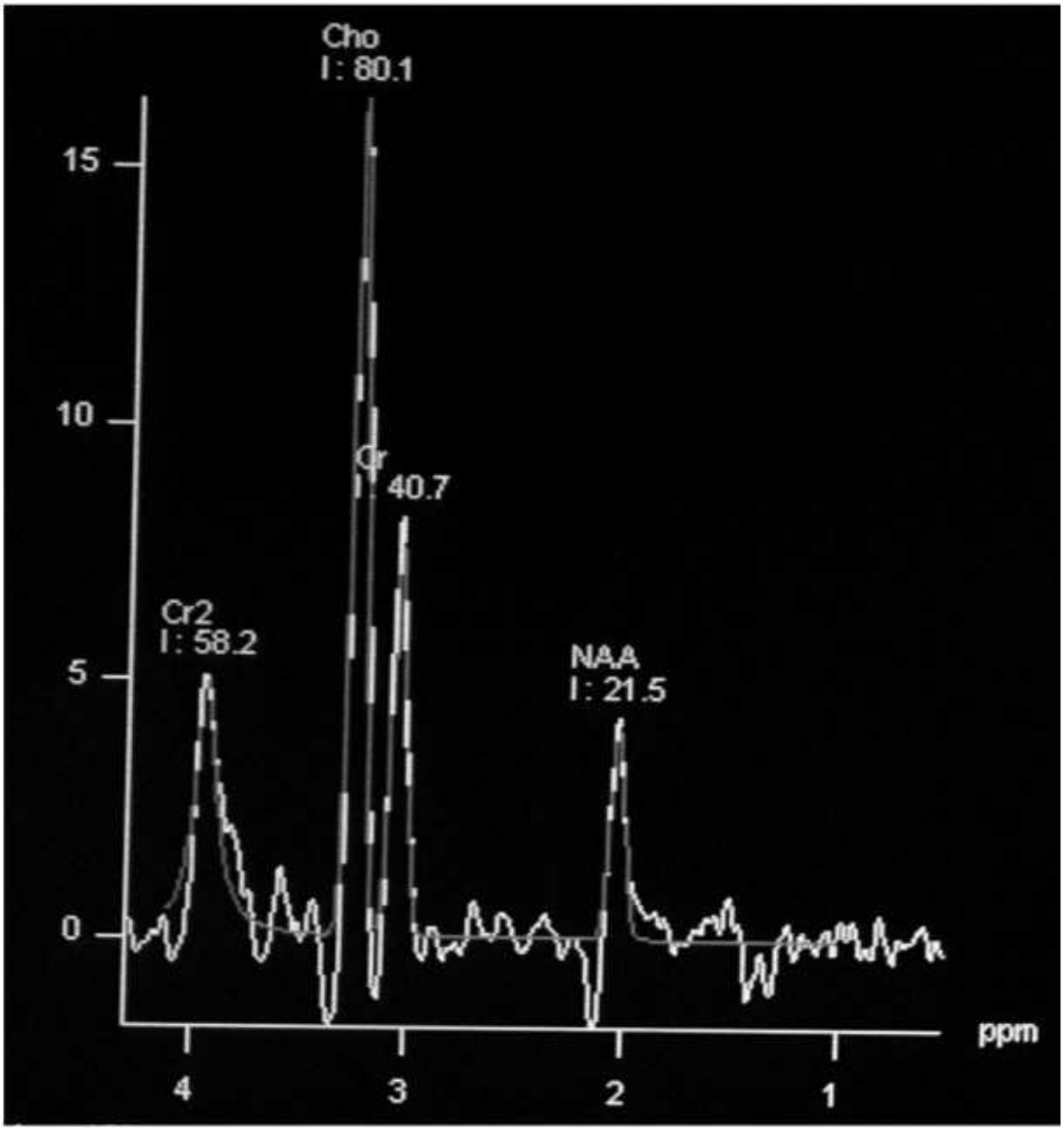


**Figure 1:** The above image illustrates the $H^1$MRS spectra acquired at intermediate TE (135ms) shows elevated choline at 3.2 and a decreased NAA peak at 2.02, presence of an inverted lactate peak at 1.3 indicates anaerobic metabolism.

Presence of elevated myo-inositol (mI) at 3.56 is observed here. Such a spectra correlates well with the possibility mentioned above as less aggressive metabolism on MRS corresponds to a moderate to low grade (WHO) tumour with elevation of mI correlating to possibility of an oligodendroglia tumor.

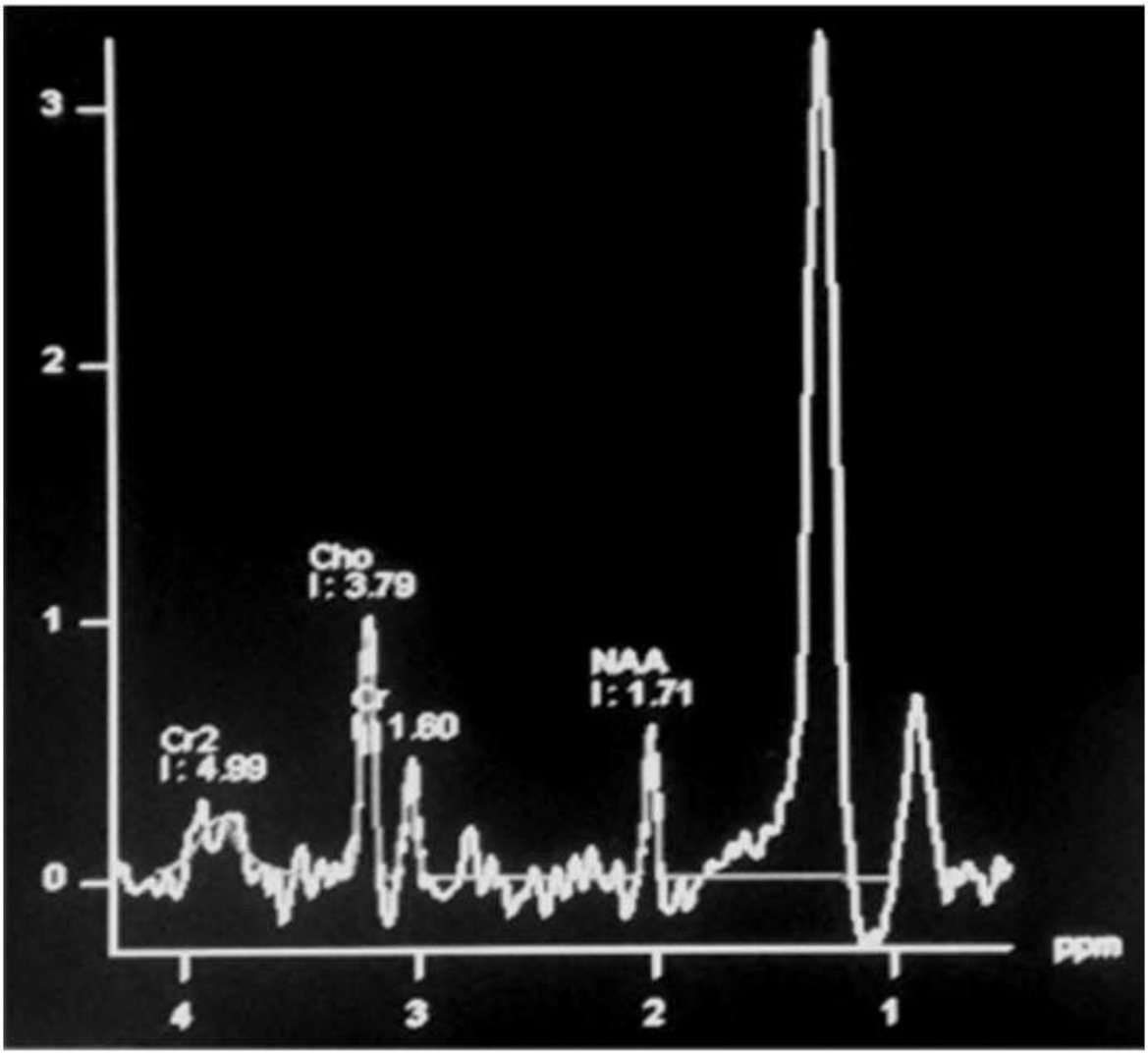


**Figure 2:** The above image illustrates the $H^1$MRS spectra acquired at intermediate TE (135ms) shows a spectra with an elevated choline at 3.2 and a decreased NAA peak at 2.02. A prominent lipid peak at 1.3 in the presence of choline in a tumor indicates a possibility of lymphoma.[20]

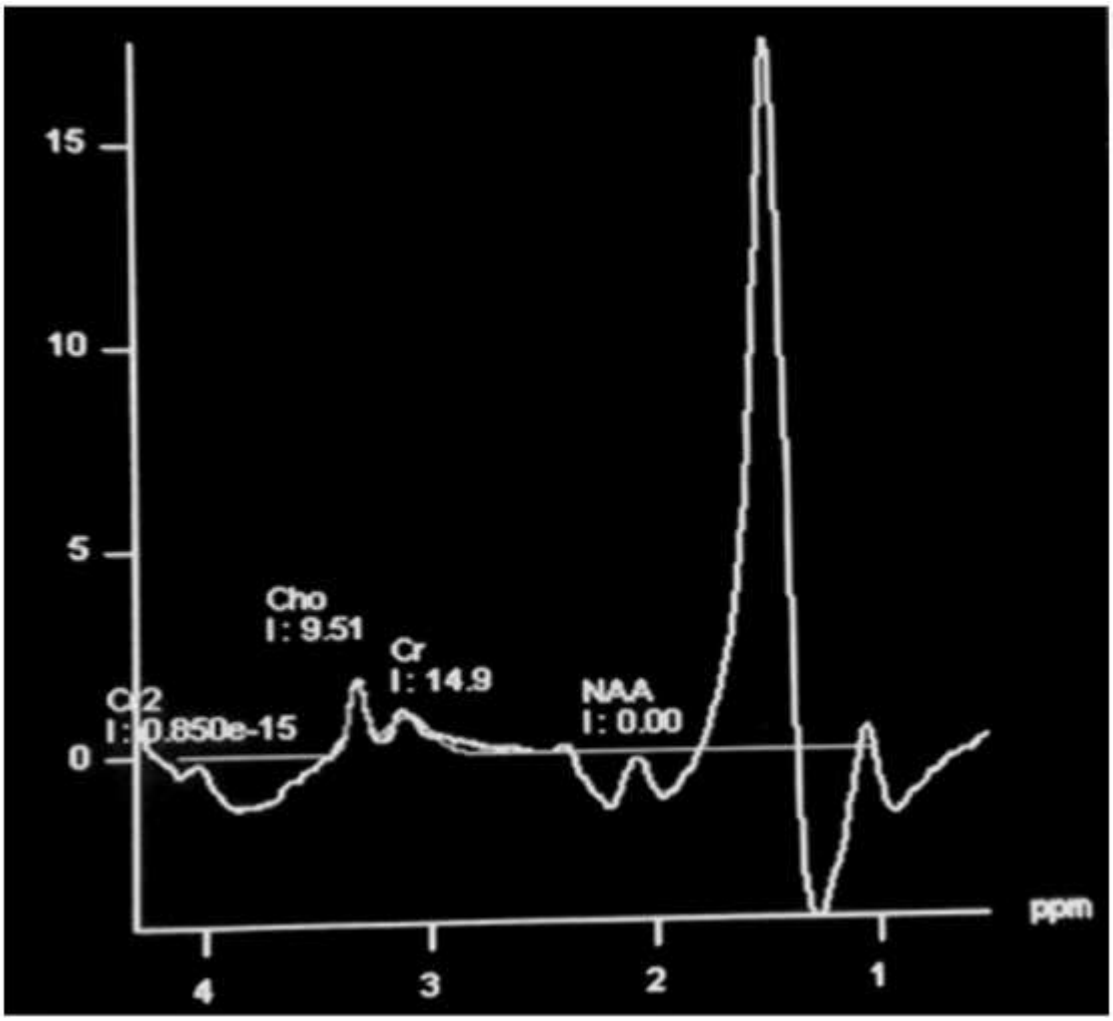


**Figure 3:** The above image illustrates the $H^1$MRS spectra acquired at intermediate TE (135ms) in a follow up case of glioblastoma multiformis showing a prominent lipid peak at 1.3 ppm. No other significant peak is seen. Such a spectra in a post-therapy scenario remains quite specific and help in differentiating an area of radiation necrosis from tumor recurrence.[20]

## LIMITATIONS OF MRS

MR spectroscopy is a technique with elegant physical principles and clinical extrapolations yet it suffers with certain inherent limitations. Physiological and non-physiological motion in human body causes an increased line width, overall frequency shifts, reduced peak areas, and decreased quality of water suppression. These in turn

lead to signal degradation and diminution and a resulting noisy spectrum which remains inappropriate for clinical interpretation.

Parallel imaging techniques with motion correction/compensation would go a long way to overcome the problem.

Field in-homogeneities due to intrinsic means the patient related factors and extrinsic, hardware related factors are reflected in the spectra as overlapping peaks. This causes poor peak identification and quantification.

The issue can be addressed by better active and passive shimming and by improving the overall field strength of the basic magnet. Truncation artifacts or sinc wiggles remain a major problem both in routine sequences as well as MRS.

This causes baseline undulations to increase to an extent of masking the peak. Better receiver systems in RF antennae however can improve upon this limitation.

Micro-metabolites and metabolites with very short signal decay time are difficult to pick up on clinically available scanners and mandate very high field strength magnets and gradient systems for detection.[30-32]

## ARTERIAL SPIN LABELING MRI[33]

The goal of ASL MRI perfusion is to produce a “flow labeled image or tag image” and a “control image” in which the static tissue signals are identical, but the magnetization of the inflowing blood is different. [33,34]

- In this technique, arterial blood water is magnetically tagged before it enters the tissue of interest. This is performed with a radiofrequency (RF) pulse that

inverts or saturates the water protons in flowing blood supplying the imaged region.[35]

- By adding a delay between labeling and image acquisition, called inversion delay (TI) in pulsed ASL (PASL) or post-labeling delay (PLD) in continuous ASL (CASL), labeled blood is allowed to reach the capillaries where it gives rise to perfusion signal.[36]
- The magnetic tracer decays with the longitudinal relaxation rate T1 and the relaxation time for water in blood or tissues is about 1- 2 s, thus only small amounts of arterial spin-labeled water accumulate in the brain.
- ASL signal-to-noise ratio (SNR) is inherently low, because the signal from the labeled inflowing blood is only 0.5%-1.5% of the full tissue signal.[33] This signal depends on many parameters, such as flow, T1 of blood and tissue, as well as the time it takes blood to travel from the site of labeling to imaging region.[37]
- Subtraction of labeled images from control images eliminates static tissue signal and the remaining signal is a relative measure of perfusion proportional to cerebral blood flow (CBF). Multiple labeled-control image pairs are acquired and averaged for the generation of CBF maps.[30,36]
- The temporal resolution is also inherently poor. The low SNR combined with the poor temporal resolution results in a low contrast-to-noise ratio (CNR). A repetition time (TR) of 2 s or more is typically used in ASL experiments. Therefore, one tag and control image pair are acquired every 4 s. A typical acquisition lasts between 5 and 10 min. [33]

Different approach;

Another approach for increasing SNR in ASL is the use of a phase array receiver coil, which can be optimized for parallel imaging to shorten the image acquisition time. Although there is usually reduction in SNR with parallel imaging, in ASL perfusion much of this SNR cost can be regained through shortened TE along with reduced distortion from susceptibility artifacts.[38]

High magnetic field strength is also beneficial for ASL, not only does image SNR increase but T1 also lengthens, allowing more spin label to accumulate.[38,39]

Since ASL is a **subtraction technique**, it is **highly sensitive** to subject movement. Filters have been developed to detect and discard bad subtraction pairs related to large movements or transient hardware gradient malfunctions. However, the best way to ensure a proper subtraction of labeled from control scans is to use fast imaging techniques, such as spiral or EPI.[33]

**TECHNIQUES FOR ASL**

1. **CASL:** CASL uses long and continuous RF pulses (2-4 s) in combination with a slice-selective gradient to induce a flow-driven adiabatic inversion of the arterial magnetization in a narrow plane of spins, usually just below the imaging plane. Major drawback is it takes longer time.[40,41]

2. **PASL:** Instead of labeling blood as it flows through a plane, as used in CASL, PASL uses short RF pulses (5 to 20 ms to saturate or invert a thick slab (10-15 cm) of blood volume, known as a tagging region, proximal to the imaging region.[33,42,43]

3. **PCASL:** PCASL has been introduced as an intermediate means to take advantage of CASL's high SNR and PASL's higher tagging efficiency. First developed by Garcia and colleagues. Here, train of discrete RF pulses together with a gradient wave applied between two consecutive RF pulses to mimic CASL's flow-driven adiabatic inversion method for spin labeling.[36,44]

4. **VSASL:** In VS-ASL, arterial spins are labeled everywhere (including in the volume of interest) based purely on flow velocity, therefore eliminating the effect of the transit delay time necessary for the labeled blood to reach a region of interest.[33,36]

**OTHER EMERGING TECHNIQUES[33]**

- Territorial ASL
- ASL at multiple Tis
- Perfusion based functional MRI

**CLINICAL APPLICATION OF ASL**

1. **To identify and differentiate the physiological region hyper-perfusion:** Regional increased signal intensity may occur in both occipital lobes corresponding to visual cortex activation. A hyper frontal pattern of regional CBF distribution has also been described with various perfusion methods. It is believed to be a normal finding in young and middle-aged patients and may decrease with normal aging.

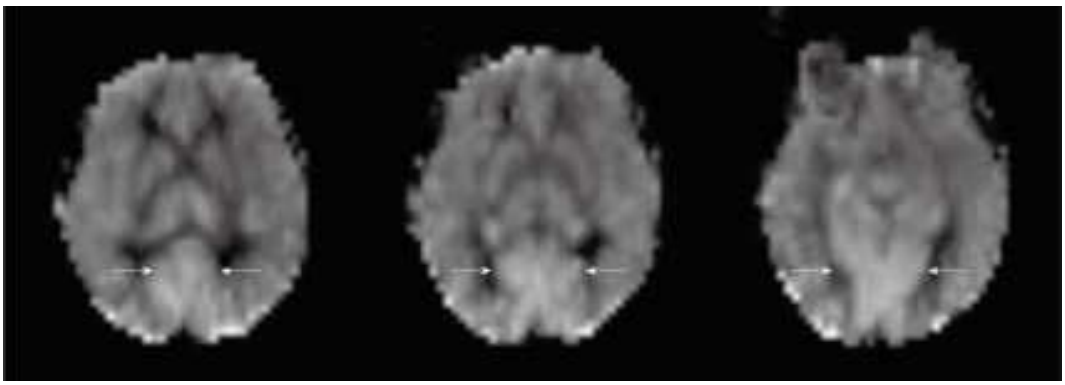

**Figure 4: Physiological hyper-perfusion in bilateral occipital cortex[33]**

1. **Age dependent variability of cerebral perfusion:** ASL can demonstrate age dependent cerebral perfusion if a quantitative measurement is used. In paediatric patients undergoing ASL, a consistent pattern of increased SNR, as well as globally elevated absolute CBF, has been observed compared with adults. This is possibly because there is a pediatric higher baseline CBF, faster mean transit time, and increased T1 values in blood and tissue.

Pediatric CBF measurements begin at a low level in the perinatal period, increase to a peak at 3-8 years of age and then gradually decrease to adult levels. After approximately age 30 years, there is a gradual decline in grey matter perfusion. Age-dependent decreases in perfusion signal intensity are well documented and must be accounted for when interpreting ASL perfusion in older patients.[46,47]

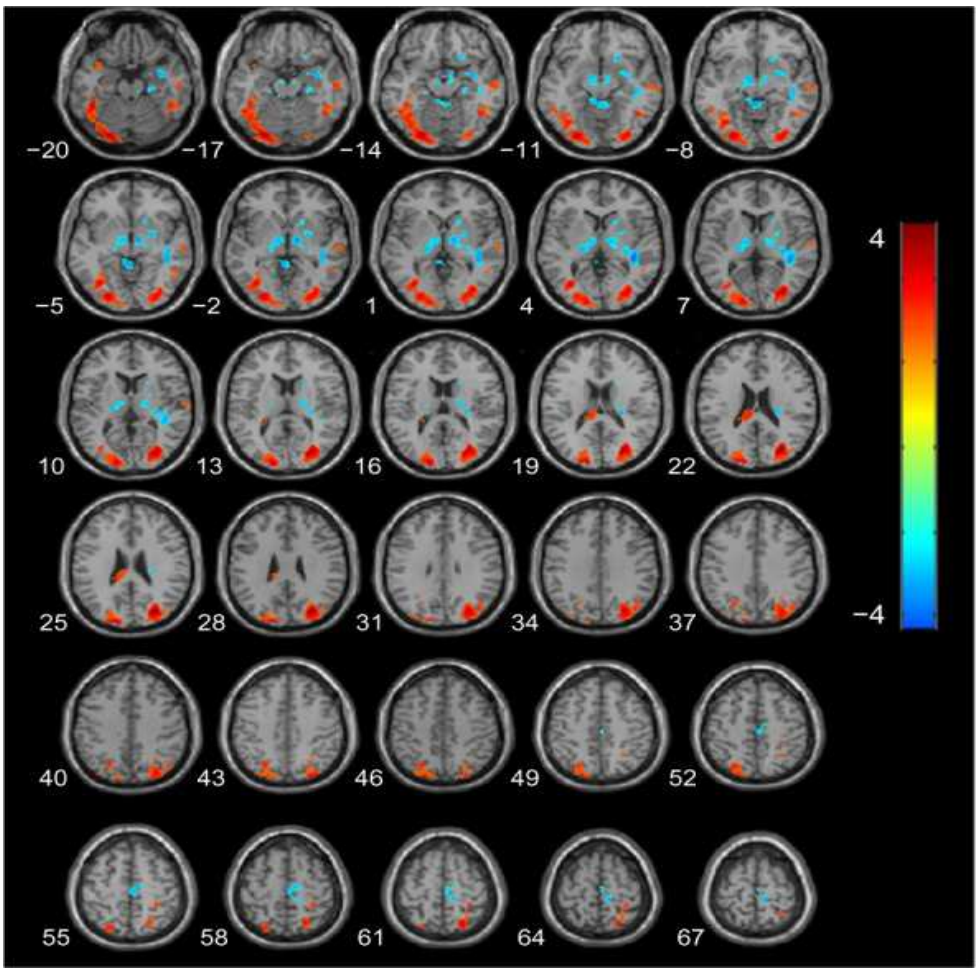


**Figure 5: Statistical parametric map of significant cerebral blood flow differences between Alzheimer's and control patients.[48]**

In the above image, Z axial coordinates in the Talairach space are from 20 to 67 mm, in increments of 3 mm. An AlphaSim correction was applied to the threshold significance level ($P$<0.05). Red = hypoperfusion, and blue = hyperperfusion, in AD.

1. **White matter signal analysis:** Gelderen et al and Osch et al had evidenced that the ASL is sensitive enough to detect WM perfusion signal and perfusion deficits. Till then ot was believed that ASL is not the better diagnostic of choice to find out the perfusion in WM.[49,50]

2. **To determine the cerebrovascular disease:** Decreased cerebral perfusion is the common underlying cause of all ischemic strokes and is a predictor of recurrent stroke. The perfusion-diffusion mismatch concept is widely used in MR imaging for ischemic acute stroke. By definition, the ischemic penumbra is an area of reduced perfusion without restricted diffusion. Also, will be helpful in determining the various cerebrovascular diseases based on the delayed arterial transit effects.[51]

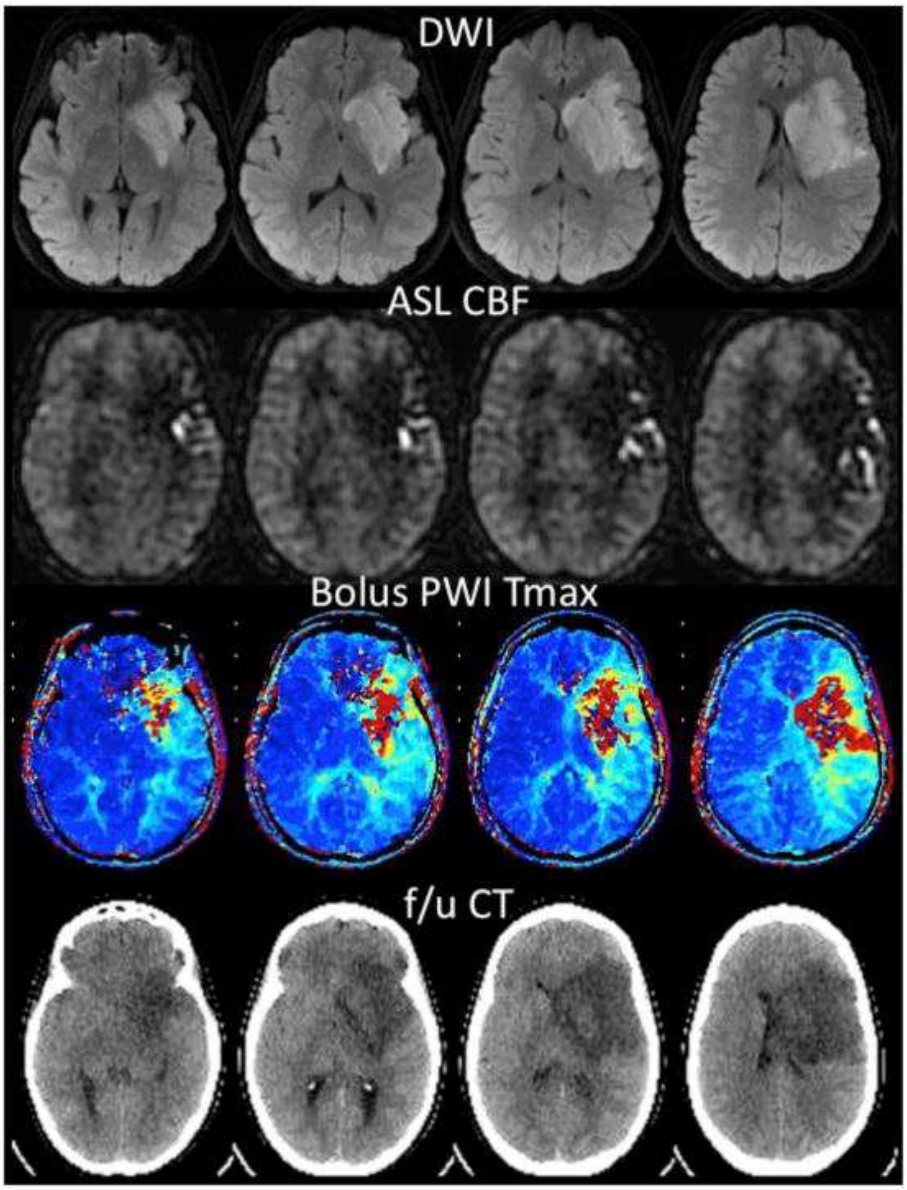


**Figure 6: ASL illustrating cerebral blood flow from a patient by Zaharchuk G et al[52]**

The MRI mentioned in the image is of 25-year-old woman 6 hrs following aortic coarctation repair and inability to speak or move her right side. MR angiogram (not shown) demonstrated no flow-related enhancement in the left middle cerebral artery (MCA). Diffusion-weighted images (DWI) confirm acute ischemic stroke in the left MCA territory. ASL CBF images show hypoperfusion in the regions with high DWI signal, with arterial transit artifact (ATA) in the periphery. Bolus contrast normalized time-to-maximum (Tmax) maps show a severe abnormality in the regions corresponding to the DWI lesion, with a milder abnormality in the region of ATA on ASL. The patient received no treatment due to her recent surgery. Coregistered slices from a follow-up noncontrast CT examination 3 days later reveals that there was no increase in the size of the lesion into the region with ATA on ASL. This is consistent with prior reports suggesting that ATA may reflect the beneficial effects of collateral flow and that such tissue has a good prognosis.

1. **Vascular malformations:** Arteriovenous malformations (AVMs) are vascular malformations with arteriovenous shunting. AVM nidus and draining veins may appear as high signal intensity on ASL perfusion maps representing AV shunting or rapid transit. The presence of hemorrhage or embolic material may produce dark signal due to susceptibility artifacts. Small AVMs may be difficult to detect with any other technique, particularly in an acute setting when hemorrhage is present.

ASL can provide evidence of AV shunting, which may be the clue for detecting subtle lesions. Perfusion abnormalities in regions adjacent to AVMs reflect various states of hyperemia and/or steal phenomenon. Developmental venous anomalies (DVAs) are frequently identified in contrast brain MRI. DVAs and their surrounding

parenchyma may show increased CBF, CBV, MTT and TTP on DSC MRI perfusion studies.

Increased perfusion in the brain parenchyma adjacent to the DVAs also can be demonstrated on the ASL perfusion maps.[53,54]

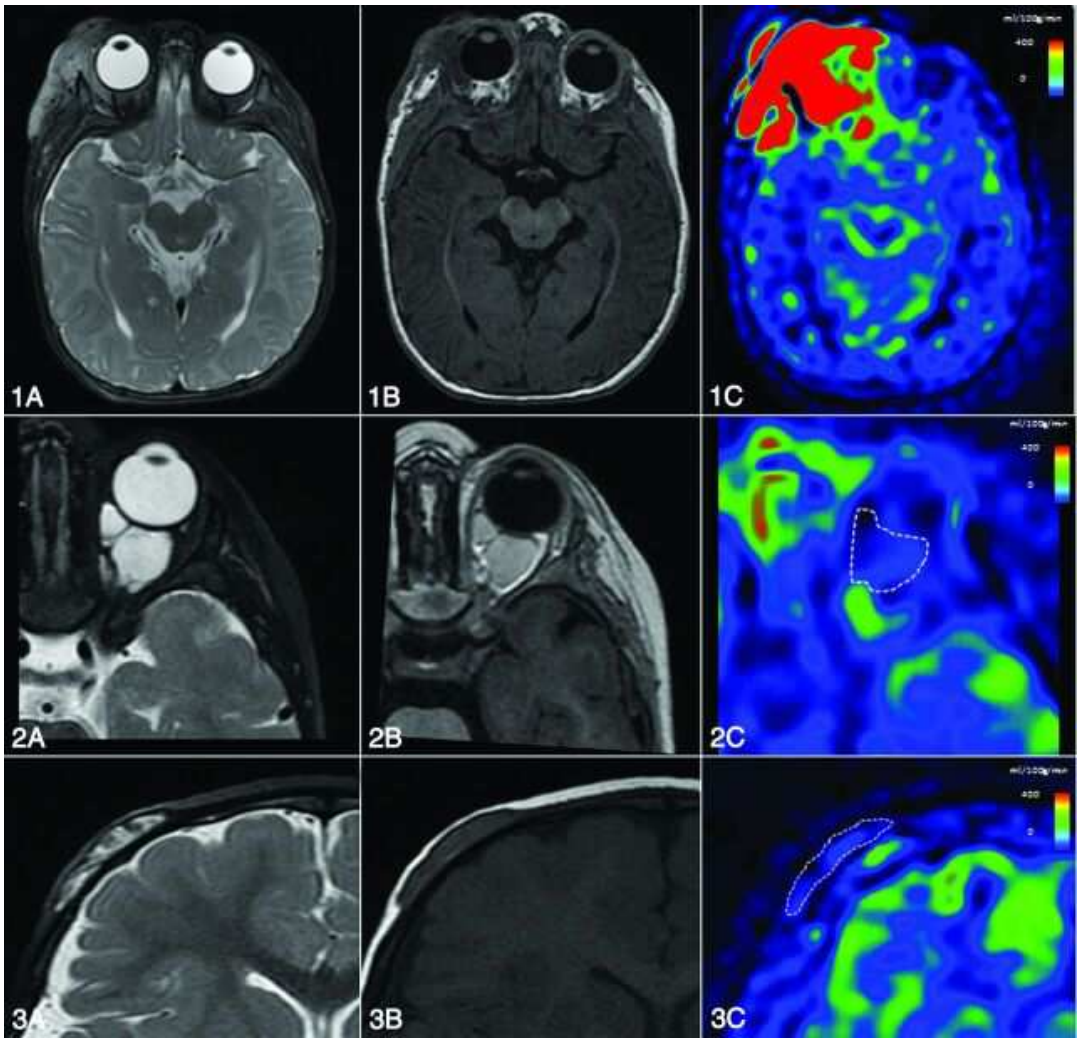


**Figure 7: Soft tissue vascular anomaly found in 13-month-old child[55]**

Illustrative cases of blood flow differences in major subtypes of STVA. Blood flow measured with ASL helps distinguish vascular anomalies. *A–C*, T2, T1, and ASL sequence blood flow maps. 1) Right intra- and periorbital haemangioma in a 6-month-old boy. ASL flow map demonstrates major lesional hyperperfusion (blood flow = 477 mL/100 g/min). 2) Intraorbital venous malformation of a 14-month-old boy with

low blood flow (67 mL/min/100 g). 3) Intraosseous cystic lymphangioma of a 13-month-old girl with a low blood flow (45 mL/min/100 g).

1. **Dementia and other cognitive disorders:** In cognitive disorders, imaging modalities are becoming increasingly important for differential diagnosis, for monitoring disease progression, and as surrogate markers in treatment trials. Besides PET and SPECT, several MRI techniques, including anatomic or volumetric imaging, BOLD fMRI, MR perfusion and diffusion tensor imaging, are currently being used for these purposes. [56,57]

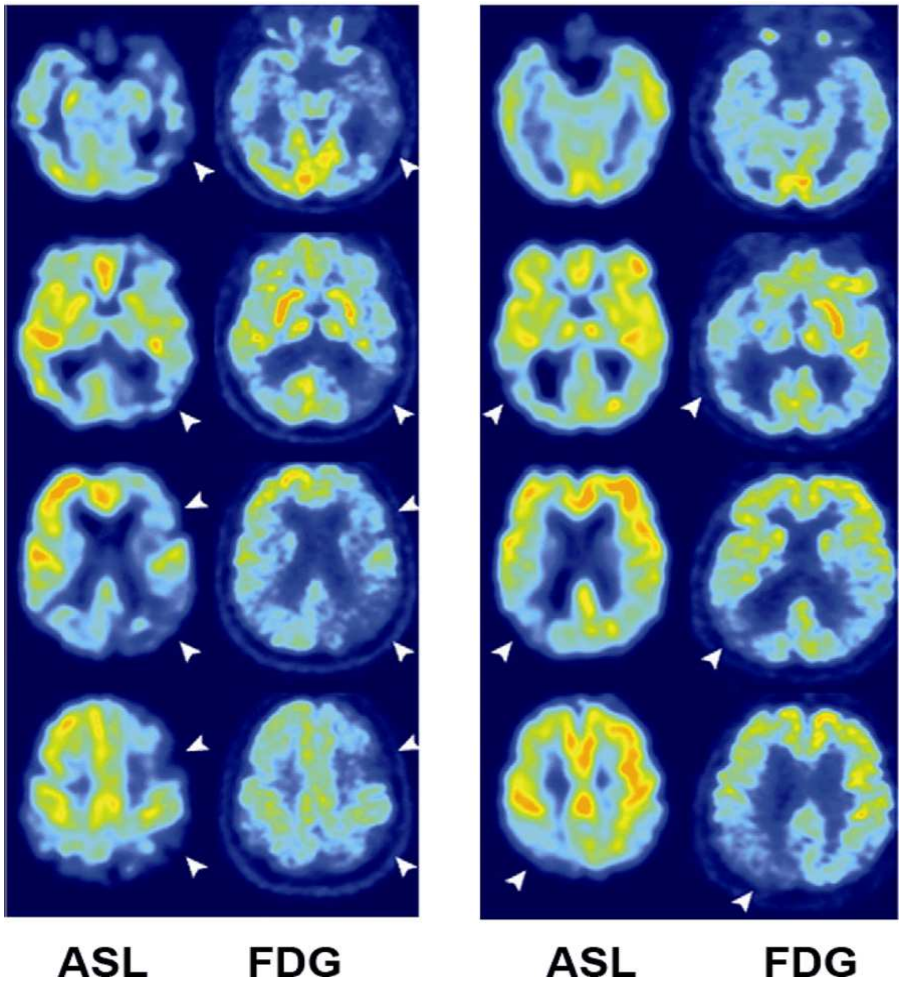


**Figure 8: Representative images from two patients with AD** comparison of ASL MRI and FDG PET. White arrows highlight areas of concordant hypoperfusion on ASL MRI and hypometabolism.[58]

1. **Epilepsy:** Epileptic foci have been studied extensively using nuclear medicine techniques. These methods require an ictal and a subsequent interictal injection of radiotracer.

Assessment of tissue metabolism is standard practice in epilepsy pre-surgical work-up with the assumption that the epileptogenic focus is abnormal tissue that has a decreased metabolic rate and blood flow between seizures and increased metabolism and blood flow during seizure activity. The hypoperfusion interictal pattern is probably related to neuronal loss but the mechanism of ictal hyper perfusion is not completely understood. It may be related to transient loss of autoregulatory function in the surrounding vasculature or to the release of excitatory neurostimulators in areas of increased neuronal activity.[59,60]

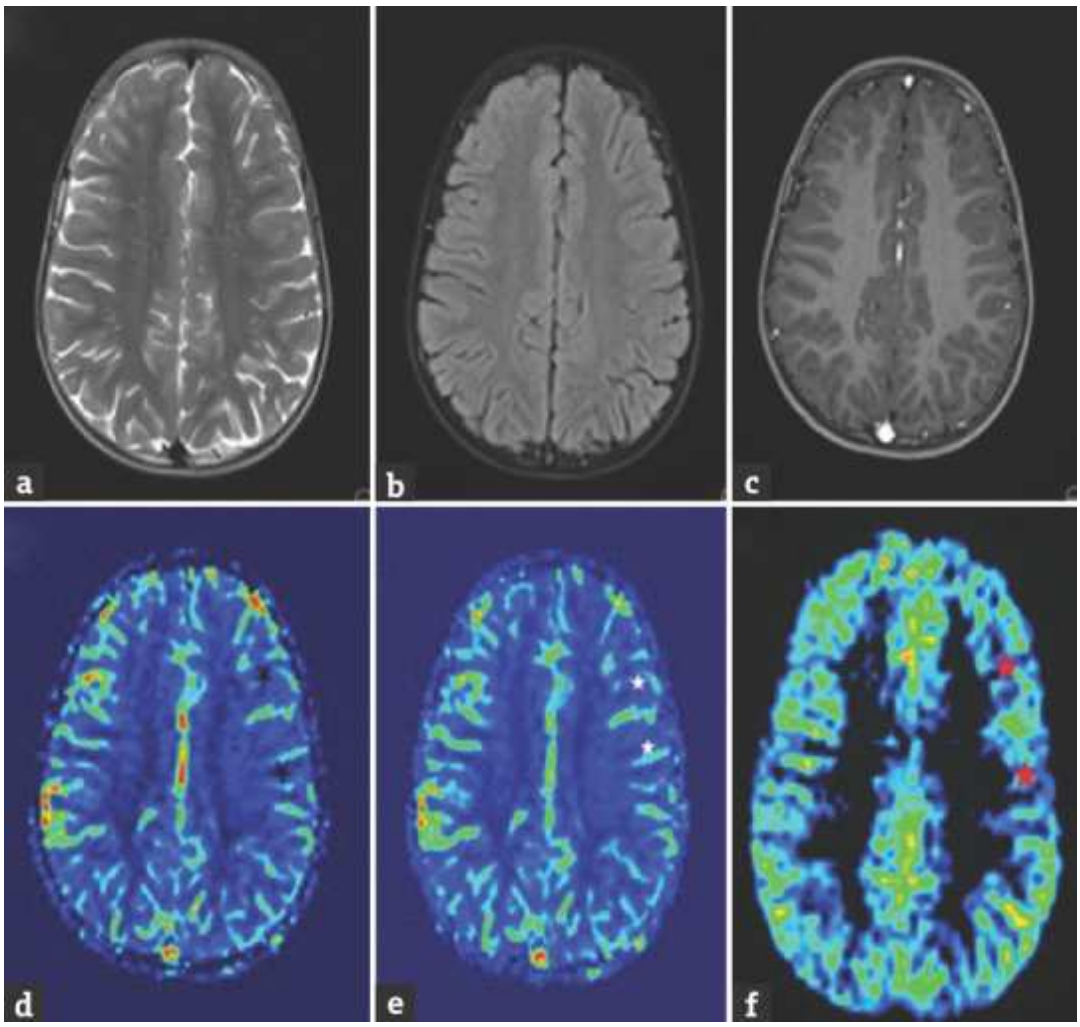


**Figure 9:** Magnetic resonance imaging of 11-year-old male child obtained 13 h after seizure onset showing no abnormality on axial T2 (a), fluid inversion recovery (b), postcontrast – T1 (c) while revealing hypoperfusion in left frontoparietal lobe on dynamic susceptibility contrast – cerebral blood volume ([d] black asterisk), dynamic susceptibility contrast – cerebral blood flow ([e] white asterisk) and arterial spin labeling ([f] red asterisk)[60]

1. **CNS infections:** Recent scholar articles suggest that most of the CNS infections demonstrate ASL hypoperfusion, but they also found some infections presented with hyperperfusion, such as herpes encephalitis. One diagnostic dilemma in immunocompromised patients is differentiating

toxoplasmosis from lymphoma. In the same study, the authors found that ASL hypoperfusion was seen in toxoplasmosis while hyperperfusion was seen in lymphoma.

Cerebral abscesses show decreased perfusion in the lesion itself as well as in the surrounding edema, however the enhancing rim can demonstrate increased perfusion signal intensity. Cortical hyperperfusion was also reported in epidural abscesses.

This might be secondary to compression of the cortical venous outflow or malfunction of the local cerebral regulatory mechanisms secondary to infection.[33,45]

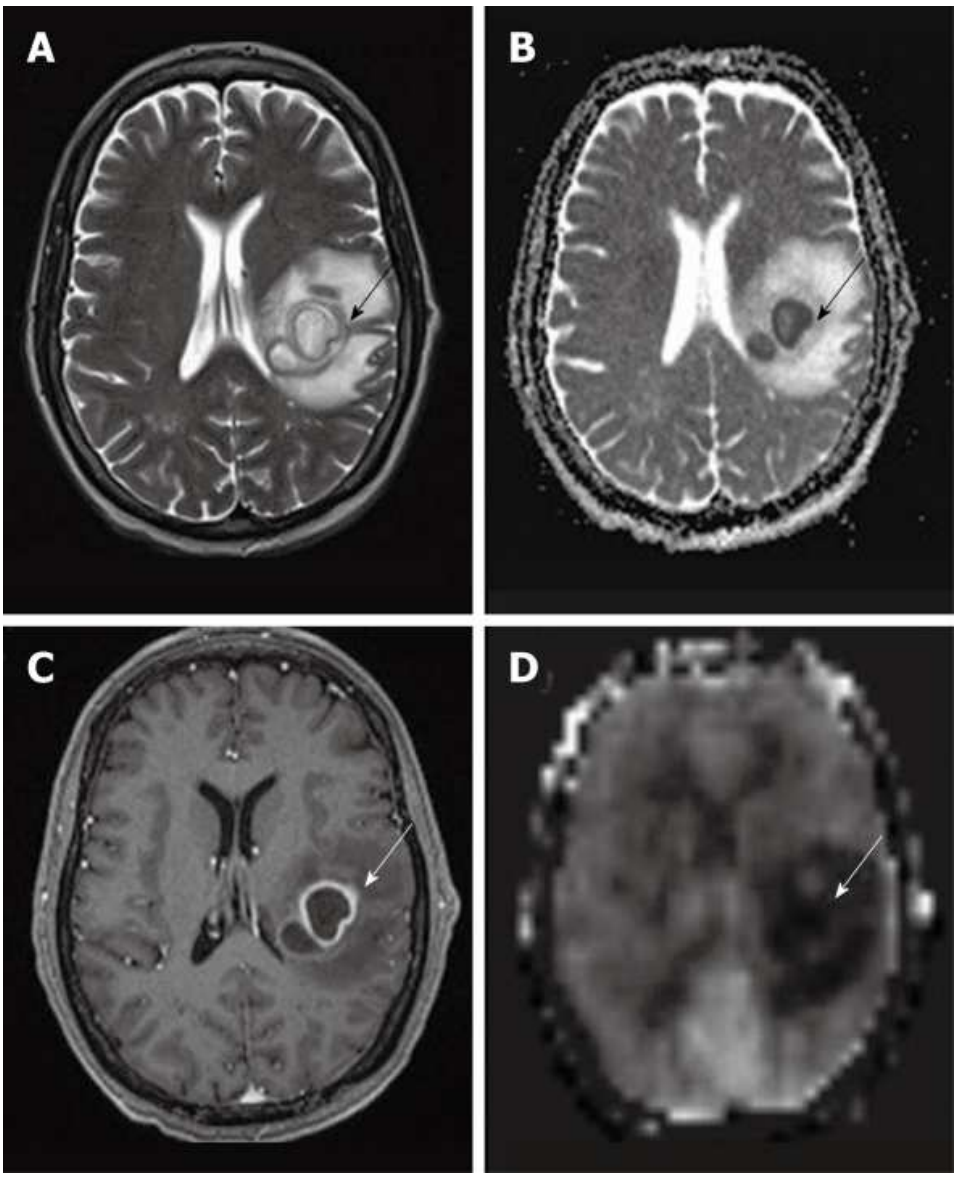


**Figure 10:** A case of abscess in the left frontoparietal lobe. T2WI (A) shows internal high signal intensity with peripheral dark signal intensity (black arrow). ADC map (B) shows low signal intensity of the abscess content, representing restricted fluid diffusion (black arrow). Smooth rim enhancement is noted on post gadolinium T1WI (C) (white arrow). An arterial spin labeling cerebral blood flow map (D) shows hypoperfusion with minimal hyperperfused rim (white arrow).[33]

1. **Neoplasms:** MR perfusion studies in the setting of CNS neoplasms are commonly performed with a DSC technique, focusing on relative cerebral blood volume (rCBV) which has been shown to correlate with tumor grade and histologic findings of increased vascularity. Perfusion imaging can be used as such to assess tumor grade, heterogeneity, and to target stereotactic biopsy sites at the most malignant portion. Perfusion evaluation in treated tumors also provides a non-invasive indicator of malignant progression or treatment response.

- Several studies demonstrated that DSC and ASL perfusion are comparable for distinction between low grade (WHO grades I and II) and high grade (WHO grades III and IV) glioma.
- A good correlation between ASL and DSC imaging for determination of relative tumor blood flow (rTBF) has also been observed.
- In comparison to DSC, ASL provides quantitative CBF values that are unrelated to disruptions of the blood-brain barrier, while DSC provides information about tumor blood volume and vessel permeability.
- To evaluate tumor response after treatment.
- In qualitative clinical interpretations, high grade primary brain tumors usually demonstrate high perfusion on ASL maps while low grade tumors usually show hypoperfusion.
- As described earlier, hypoperfusion in tumors on ASL maps must also be correlated with hemorrhage, cysts and/or calcifications, which may show artificially low signal intensity.
- Hyper perfusion is also observed in meningiomas, oligodendrogliomas, hemangioblastomas and glomus tumors.

- Metastases can demonstrate either hypo- or hyper perfusion patterns on ASL maps.[33]

Fu M et al had conducted a Meta-analysis in which they had found 346 lesions from 346 patients, 274 were high-grade gliomas (HGG) and 72 were brain solitary metastases (BSM). The forest pooled sensitivity of 0.88 and specificity of 0.85 of ASL were reported in this meta-analysis. Sensitivity analysis demonstrated that the pooled estimates were reliable. No evident publication bias was obtained. Hence, they concluded that parameters derived from ASL with high accuracy in differentiating HGG from BSM. However, results must be interpreted with caution due to the small sample size considered. Large sample prospective studies were necessary to assess and confirm its clinical value.[60]

Similar study by Delgado AF et al also reported that Arterial spin-labeling–derived CBF measures showed high diagnostic accuracy for discriminating low- and high-grade tumors in pediatric patients with brain tumors. The relative CBF showed less variation among studies than the absolute CBF. One of their major observations was The mean difference in aCBF showed significantly higher CBF in high grade tumors compared with low grade tumors. The mean difference for aCBF was 29.62 mL/min/100 g.[61]

Another clinical study by Alsaedi A et al had discussed in their reviw of articles that the absolute tumour blood flow (TBF) values can differentiate high-grade gliomas (HGGs) from low-grade gliomas (LGGs) and grade II from grade IV tumours. However, it lacked the capacity to differentiate grade II from grade III tumours and grade III from grade IV tumours. In contrast, the relative TBF (rTBF) is effective in differentiating HGG from LGG and in glioma grading. The maximum rTBF

(rTBFmax) demonstrated the best results in glioma grading. These results were also reflected in the sensitivity/specificity analysis in which the rTBFmax showed the highest discrimination performance in glioma grading. The estimated effect size for the rTBF was approximately similar between high grade gliomas and low-grade gliomas. Also, grade II and grade III tumours as they found negative observed values. While it exhibited smaller effect size between grade III and grade IV. Sensitivity and specificity analysis replicate these results as well. This meta-analysis suggests that ASL is useful for glioma grading, especially when considering the rTBFmax parameter.[62]

Patil YP et al aimed to analyze and identify various characteristic changes of multiple ring-enhancing lesions in the brain on conventional MRI and proton MR spectroscopy which leads to an early diagnosis, treatment, response assessment and minimize the complications in such patients. They had conducted a descriptive study, consisting of 50 patients that were suspected clinically with ring-enhancing lesions were referred to the department of Radio-diagnosis and underwent scanning in 1.5 Tesla MRI over a period of 2 years. They observed that out of 50 patients, 19 were diagnosed as neurocysticercosis, 16 as Tuberculomas, 7 as Intracranial Abscess, 4 as metastasis, 3 as primary brain neoplasms, and 1 as tumefactive Demyelination. Neurocysticercosis was found to be the most common of the pathology diagnosed with Seizures being the most common complaint in patients. Hence, they concluded that the use of MRI along with MR spectroscopy is of vital importance and primary research tool in neuro diagnosis. The most common ring enhancing lesions experienced in developing countries like India is NCC and tuberculomas. Accurate diagnosis and characteristics of these lesions can be achieved

by MR spectroscopy on a routineMRI scan by analyzing the quantity and ratio of tissue metabolites [63]

Seth R et al had reported a case of 4-year-old girl with ring enhancing lesions in brain CT, initially diagnosed as neurocysticercosis but did not respond to cysticidal therapy. A Magnetic resonance spectropscopy (MRS) revealed lipid peaks suggestive of tuberculoma which was successfully treated with antituberculosis therapy. This report highlights the role of MRS in the diagnosis of ring enhancing lesions.[64]

Similar evidence by Soni N et al had assessed the diagnostic performance of arterial spin-labeling (ASL) magnetic resonance perfusion imaging to differentiate neoplastic from non-neoplastic brain lesions. Thirty patients were in the neoplastic group, of which 15 had high-grade gliomas (HGGs), 15 metastases and 30 in the non-neoplastic group had found with 12 tuberculomas, 10 neurocysticercosis, four abscesses, two fungal granulomas and two tumefactive demyelination based on final histopathology and clinco-radiological diagnosis.

They found significantly higher nCBFL and nCBFPE values in the neoplastic group than non-neoplastic. For predicting neoplastic lesions, we found an nCBFL cutoff value of 1.89 and nCBFPE value of 0.76. Mean nCBFL was higher in HGGs was $8.70 \pm 4.16$ compared to tuberculomas $1.98 \pm 0.87$ and nCBFPE was higher in HGGs, which was $3.06 \pm 1.53$ compared to metastases which was found to be $0.86 \pm 0.34$ and tuberculomas with $0.73 \pm 0.22$, which had significant difference of $p < 0.001$. They stated that ASL perfusion may help in distinguishing neoplastic from non-neoplastic brain lesions.[65]

Another study which had evaluated the ability of cerebral blood flow (CBF)-guided voxel-by-voxel analysis of multivoxel proton MR spectroscopic imaging ($^{1}$H-MRSI) to differentiate low-grade from high-grade gliomas was conducted by Chawla S et al. In their study, A total of 35 patients with primary gliomas (22 high grade and 13 low grade) underwent continuous arterial spin-labeling perfusion-weighted imaging (PWI) and $^{1}$H-MRSI.

Different regions of the gliomas were categorized as "hypoperfused," "isoperfused," and "hyperperfused" on the basis of the average CBF obtained from contralateral healthy white matter. $^{1}$H-MRSI indices were computed from these regions and compared between low- and high-grade gliomas. Using a similar approach, they had applied a subgroup analysis to differentiate low- from high-grade oligodendrogliomas because they show different physiologic and genetic characteristics. They found that $^{1}$H-MRSI indices from the "hyperperfused" regions of gliomas, on the basis of PWI, may be helpful in distinguishing high-grade from low-grade gliomas including oligodendrogliomas.[66]

Noguchi T et al had investigated the characteristics of arterial spin-labeling magnetic resonance imaging (ASL-MRI) in central nervous system (CNS) infection. Among the 17 patients with non-purulent parenchymal involvement, ASL-MRI revealed high perfusion in 8 patients (47%) and low perfusion 1 patient (6%). Especially, four of five patients (80%) with definite or suspected herpes simplex virus (HSV) infection showed high perfusion on ASL-MRI.

Seventeen of 22 patients (77%) with meningeal involvement showed high perfusion along the cerebral sulci irrespective of the pathogens. Meanwhile, 4 of 16 lesions (25%) with abscess formation showed low perfusion and one of six patients

(17%) with ventricular involvement had high perfusion. Hence, they concluded that The characteristics of ASL-MRI in CNS infections were clearly delineated. ASL-MRI could be helpful for monitoring the brain function in CNS infections noninvasively.[67]

# MATERIALS AND METHODOLOGY

The present study was conducted by including the patients showing ring enhanced lesions on MRI Scan presenting to the department of Radio-diagnosis at KLE' Dr. Prabhakar Kore Hospital and MRC, Belagavi.

**Study design:** Cross-sectional, observational study.

**Study period:** One year, 1st Jan 2021 to 30th December 2021

**Study setting:** KLE' Dr Prabhakar kore Hospital and MRC, Belagavi.

**Sample size:** By applying the formula for sample size calculation,

$N = z_\alpha^2 P(1-p)/d^2$, where $z_\alpha$ is the constant, p is the prevalence from previous study we obtained and d is the percentage likely difference in the prevalence. For 5% significance level, $z_\alpha$ is 1.96, the minimum sample size is 33.

**Inclusion criteria:**

1. Patients aged between 18 to 90 years
2. Patients of both genders detected with single or multiple ring enhancing lesions of MRI Brain Scan, who are referred to Radiodiagnosis for ASL perfusion and MR Spectroscopy.
3. Patients willing to participate in the study by giving written informed consent.

**Exclusion criteria:**

1. Contra indications for MRI such as metallic rods/screws/foreign bodies/vascular clips/cardiac pacemakers and infusion pumps.
2. Patients not willing to participate in the study

## DETAILED METHODOLOGY

After obtaining the institutional ethics committee clearance, 35 patients with the above-mentioned inclusion criteria were included the study. The protocol, its advantages and disadvantages were explained. Written informed consent was taken. The demographic details such as age, gender, presenting complaints and the past history were noted by conducting face-to-face interview. Then all the study population were subjected for MR spectroscopy and ASL

Procedure:

- Had been told that no need of prior fasting for MRI
- On the day of MRI, the patients were instructed to change into the appropriate gown and to not have any metallic items with them
- Also, the list of most common metallic items was given as an example to make them understand.
- We had also explained about the humming/ buzzing sound that could to heard by them during the procedure.
- If the scan detected any ring enhancing lesions, the patients were subjected to Arterial spin labeling to first detect if the lesion was malignant or benign, then the patients were subjected for MR spectroscopy to rule out other lesions due to infectious cause.

**ASL perfusion:** MRI images were obtained using routine image protocols including axial T2, T1/T2 fluid attenuated inversion recovery (FLAIR), diffusion weighted imaging (DWI) and post contrast T1.

Whole brain three-dimensional pseudo continuous ASL was done.

In ASL sequencing, tagging pulses were applied to a slab of tissue proximally from the imaging volume that inverts the magnetization of water molecules in the slab. Post label delay/ inversion time-waiting for labelled blood to reach the blood parenchyma.

Imaging parenchyma was in labelled and unlabelled state.

Subtraction of labelled and control image, was eliminated static tissue- signal proportional to local CBF. Cerebral blood flow was calculated using the formula.

Preparation Module (inversion) – Continuous RF (CASL), pulsed RF (PASL), Hybrid (pCASL).

**POST PROCESSING AND DATA ANALYSIS:**

After obtaining the ASL sequencing, mosaic and splitting of sequencing was done.

Colour mapping was done and ROI was placed on the areas of interest and on the contralateral normal grey and white matter.

Cerebral blood flow was calculated by one circular areas of interest over the lesion showing highest perfusion signal seen on the CBF maps from the non-enhancing areas within 1cm from the lesion (edema): excluding the necrotic, haemorrhagic and cystic areas.

One value was taken.

Normalised CBF ratios were calculated by dividing the average CBF from lesion and PE to average CWM CBF.

**MR spectroscopy:** Steps followed were;

T2/ FLAIR to identify the area of interest, position single or multiple voxel, shim areas of interest and water suppression.

Interpretation of MR spectrum was taken from variations in the chemical ratio and concentrations, which alter the peak area for the endogenous metabolites, appearance of pathological metabolites and exogenous compounds.

## EQUIPMENT

TESLAMRI machine Skyra Magnetom Spectra manufactured by Siemens.

Standard scan protocol was followed for all the patients undergoing MRI. Once the MRI was done, films were analysed, findings were noted. If the ring enhancing lesions were observed then ASL and MR spectroscopy were done.

## MRI SEQUENCING OBTAINED

***Pre-contrast:***

T1W - Axial, sagittal T2W – Axial, Sagittal, coronal

FLAIR – Axial DWI, ADC

***Post-contrast:***

T1 – Axial, Sagittal, Coronal ASL

MR spectroscopy

# RESULTS

All the obtained observations were analysed and represented as tables and graphs below.

**Table 1: Pattern of Distribution of age**

| Age | Number of patients | In % |
|---|---|---|
| 20-29 | 5 | 14.3% |
| 30-39 | 4 | 11.4% |
| 40-49 | 5 | 14.3% |
| 50-59 | 7 | 20.0% |
| 60-69 | 11 | 31.4% |
| 70-79 | 2 | 5.7% |
| >79 | 1 | 2.9% |
| Average | 63.8±9.4 | |
| Total | **35** | |

The incidence of patients aged between 60 to 69 years were higher with the incidence of 11 (31.4%) followed by 7 (20%) aged between 50 to 59 years. Five (14.3%) each were aged between 20 to 29 years and 40 to 49 years. 4 (11.4%), 2 (5.7%) and 1 (2.9%) were aged between 30 to 39 years, 70 to 79 years and >79 years respectively. The average age of our study population was 63.8±9.4 years.

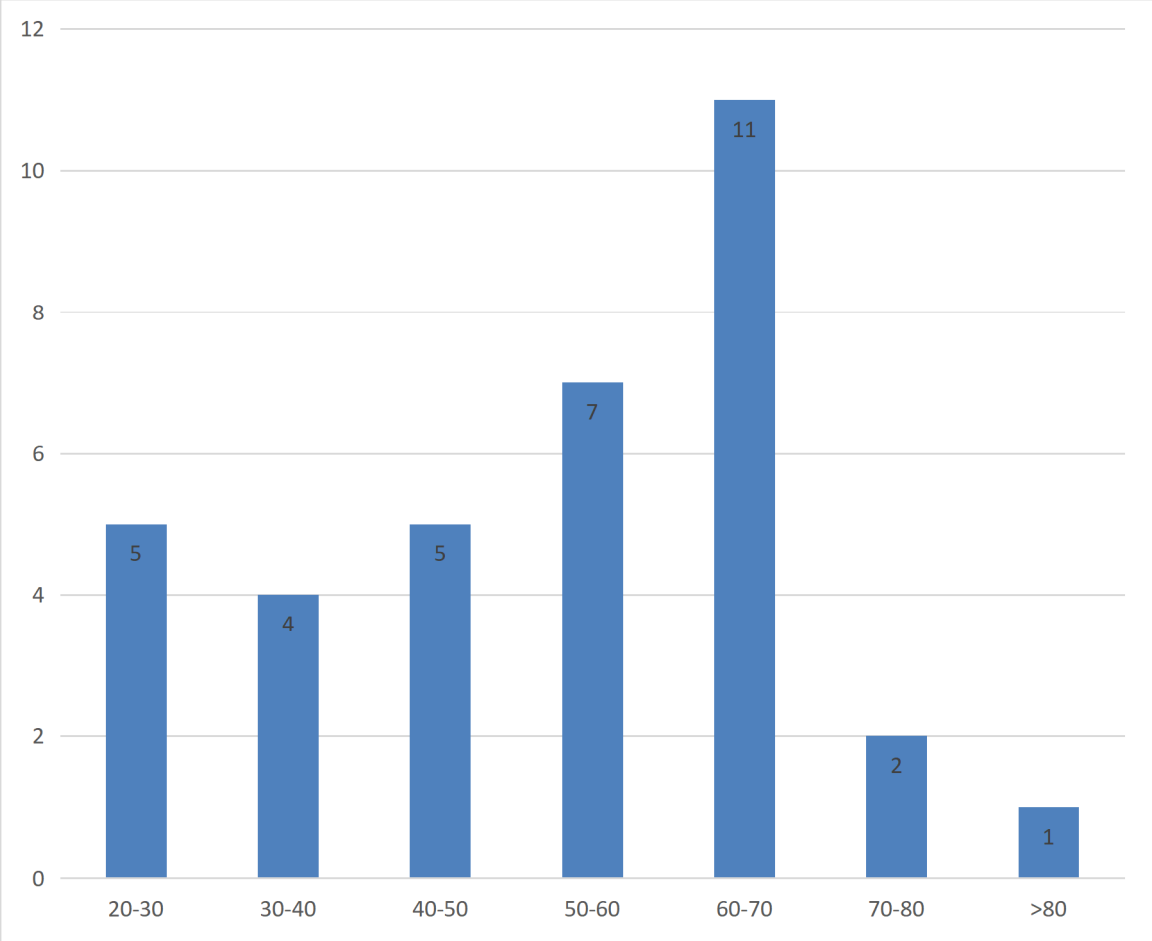


**Graph 1: Distribution of age of the study population**

**Table 2: Pattern of Distribution of gender:**

| Gender | Number |
|---|---|
| Male | 18 (51%) |
| Female | 17 (49%) |
| Total | 35 |

We found 18 male and 17 female patients in our study.

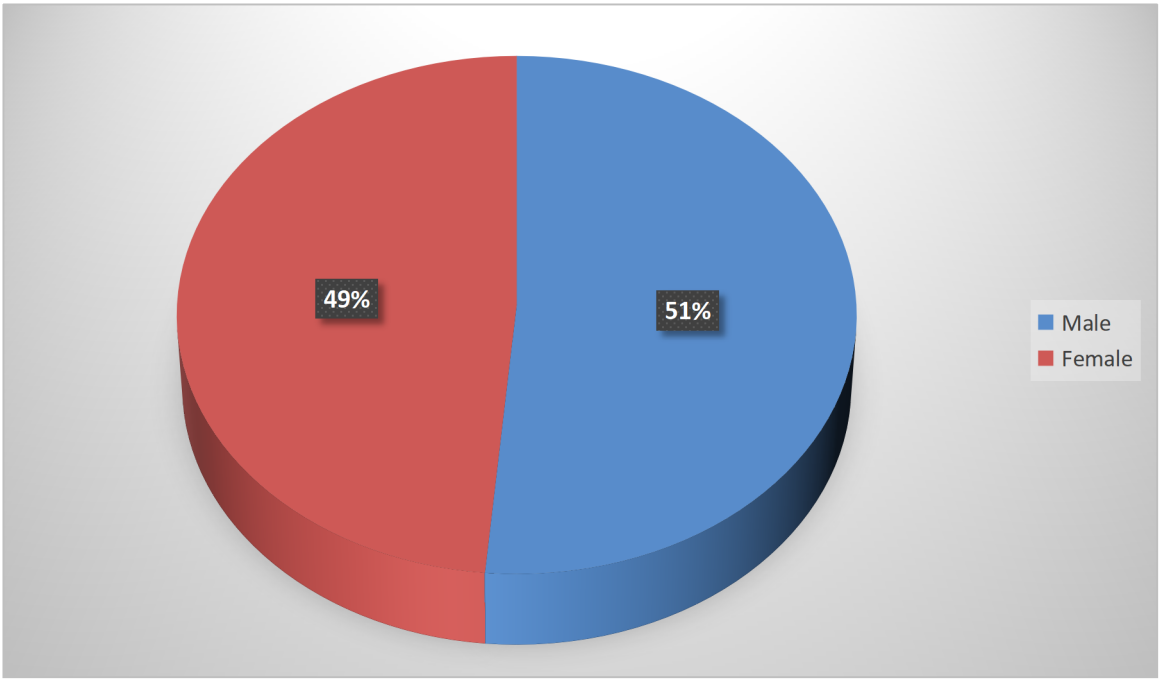


**Graph 2: Distribution of the gender**

**Table 3: Pattern of distribution of symptoms**

| Symptoms | N | In % |
|---|---|---|
| Headache | 21 | 60.0% |
| Seizures | 12 | 34.3% |
| Vomiting | 8 | 22.9% |
| Altered Sensorium | 6 | 17.1% |
| Fever | 5 | 14.3% |

We observed that 21 (60%) of the patients presented with headache followed by 34.3% (12) with seizures. 8 (22.9%), 6 (17.1%) and 5 (14.3%) had were presented with vomiting, altered sensorium and fever respectively.

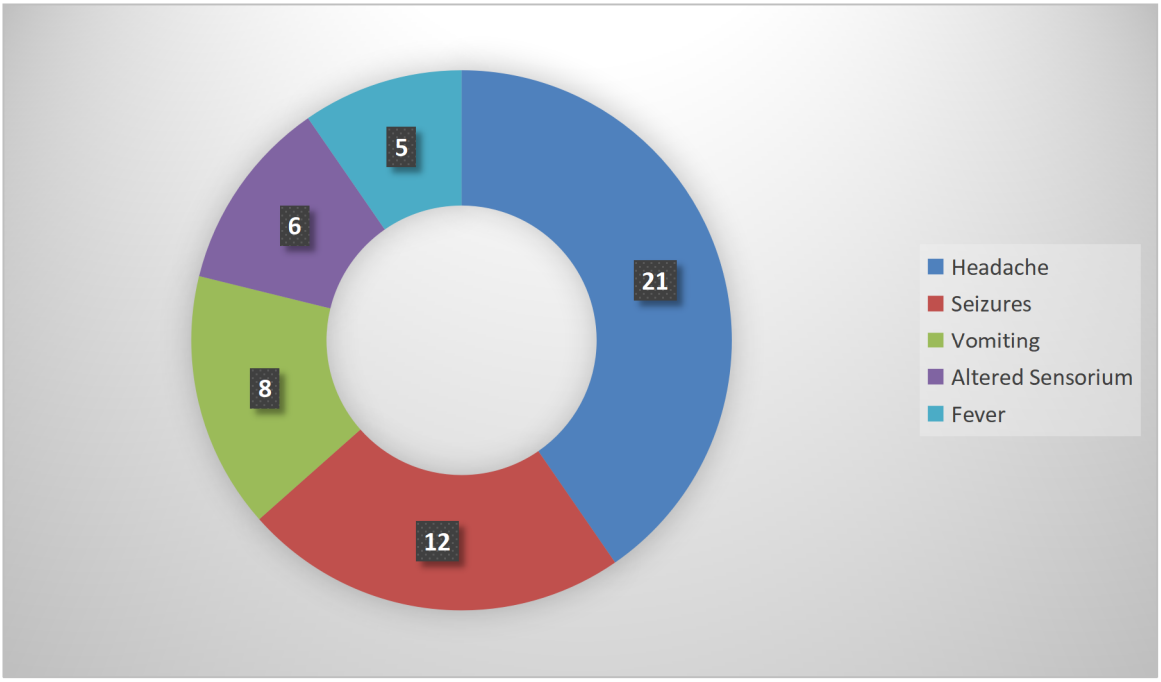


**Graph 3: Distribution of presenting complaints**

**Table 4: Pattern of distribution of T1 morphology**

| Morphology | N | In % |
|---|---|---|
| Isodense | 14 | 40.0% |
| Hyperintense | 4 | 11.4% |
| Hypointense | 17 | 48.6% |
| Total | 35 | |

The above table illustrates the T1 morphology distributed among the study population. The incidence of hypodense lesions were higher with the proportion of 48.6% (17) followed by 40% (14) with isodense and the rest 4 (11.4%) had found with hyperdense lesions.

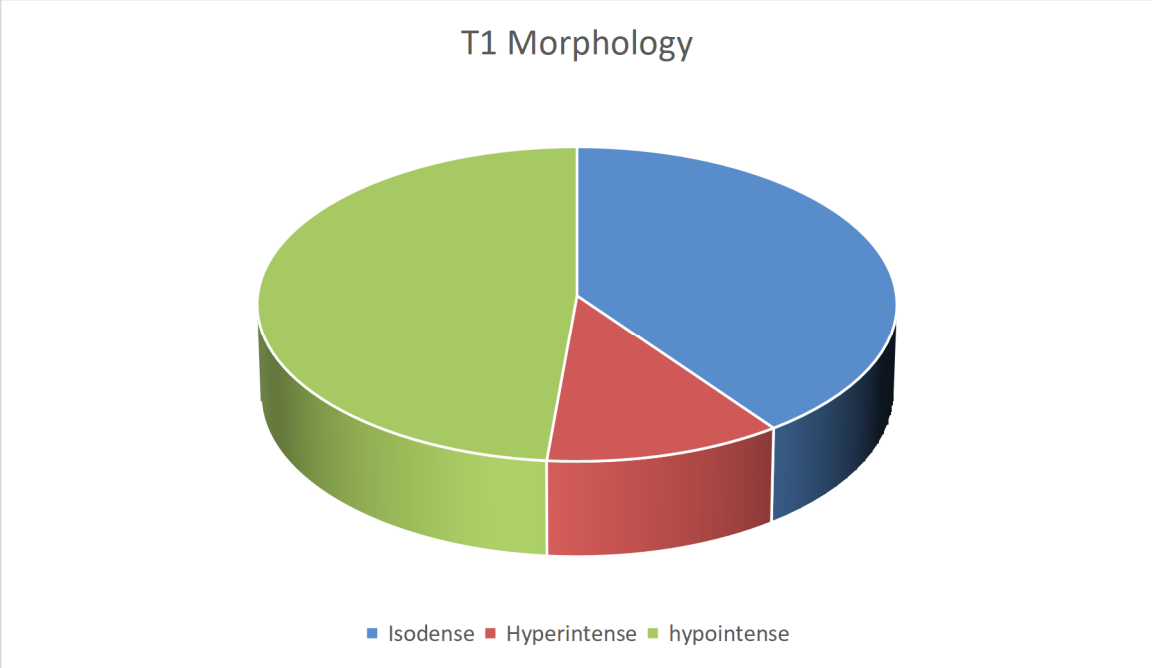


**Graph 4: Distribution of T1 imaging morphology observed**

**Table 5: Pattern of distribution of T2 morphology**

| Morphology | N | In % |
|---|---|---|
| Isodense | 4 | 11.4% |
| Hyperintense | 29 | 82.9% |
| Hypointense | 2 | 5.7% |
| Total | 35 | |

We found that 82.9% (29) patients had observed with hyperdense lesions followed by 4 patients with isodense and the rest 2 patients had hypodense lesions.

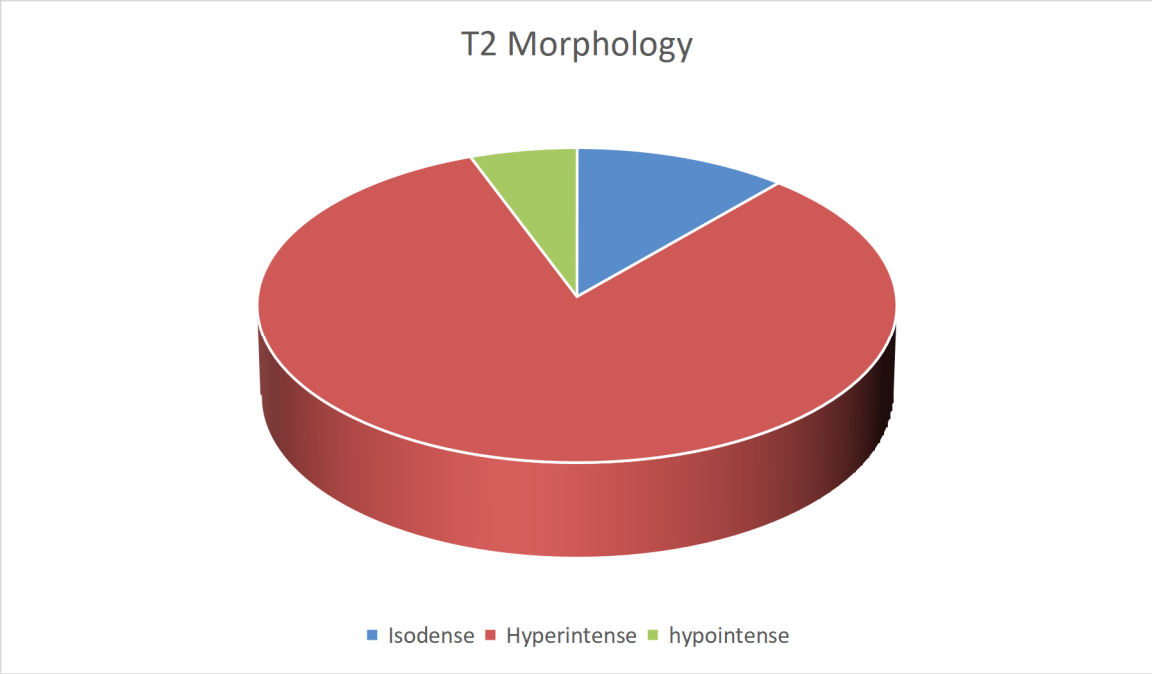


**Graph 5: Distribution of T2 morphology.**

**Table 6: Pattern of distribution of diffusion restriction**

| Diffusion Restriction | N | In % |
|---|---|---|
| Present | 25 | 71.4% |
| Absent | 10 | 28.6% |
| Total | 35 | |

With the above table we can see that diffusion restriction was found among 71.4% (25) of the study population and was absent among 28.6% (10) patients.

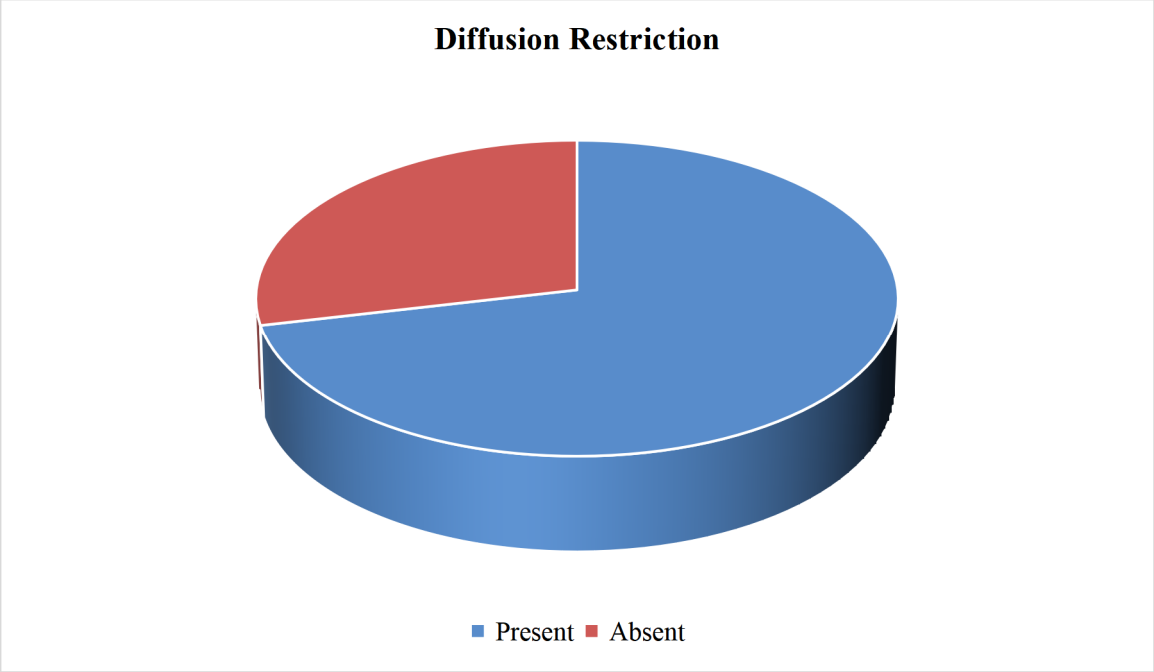


**Graph 6: Distribution of diffusion restriction**

**Table 7: Distribution of spectroscopy**

| Observation | N | In % |
|---|---|---|
| ALANINE PEAK. INCREASED AMINO ACID PEAK | 1 | 2.9% |
| CHOLINE PEAK | 7 | 20.0% |
| CHOLINE PEAK, LIPID LACTATE PEAK | 1 | 2.9% |
| CHOLINE PEAK, REDUCED NAA, ELEVATED CHOLINE CREATININE RATIO | 1 | 2.9% |
| ELEVATED CHOLINE CREATININE RATIO | 1 | 2.9% |
| LIPID LACTATE PEAK | 6 | 17.1% |
| LIPID LACTATE PEAK, INCREASED TRE | 3 | 8.6% |
| NAA PEAK | 7 | 20.0% |
| NORMAL | 1 | 2.9% |
| RAISED NAA | 2 | 5.7% |
| RAISED CHOLINE, RAISED NAA | 1 | 2.9% |
| REDUCED NAA, ELEVATED CHOLINE-CREATININE RATIO | 1 | 2.9% |
| REDUCED NAA, INCREASED CHOLIE, LIPID LACTATE PEAK | 1 | 2.9% |
| REDUCED NAA, REDUCED NAA/CR RATIO | 1 | 2.9% |
| REDUCED NAA/CR, LIPID LACTATE PEAK | 1 | 2.9% |

Choline and NAA peak were the most common finding observed with the incidence of 7 (20%), followed by lipid lactate among 6 (17.1%) of the patients included in our study.

Mean Cho/Cr and Cho/NAA ratios were 2.87±0.98 and 2.69±0.91 respectively.

Mean Cho/Cr levels were recorded as 3.38±0.72 and 3.92±0.63 for high grade tumours and metastasis respectively.

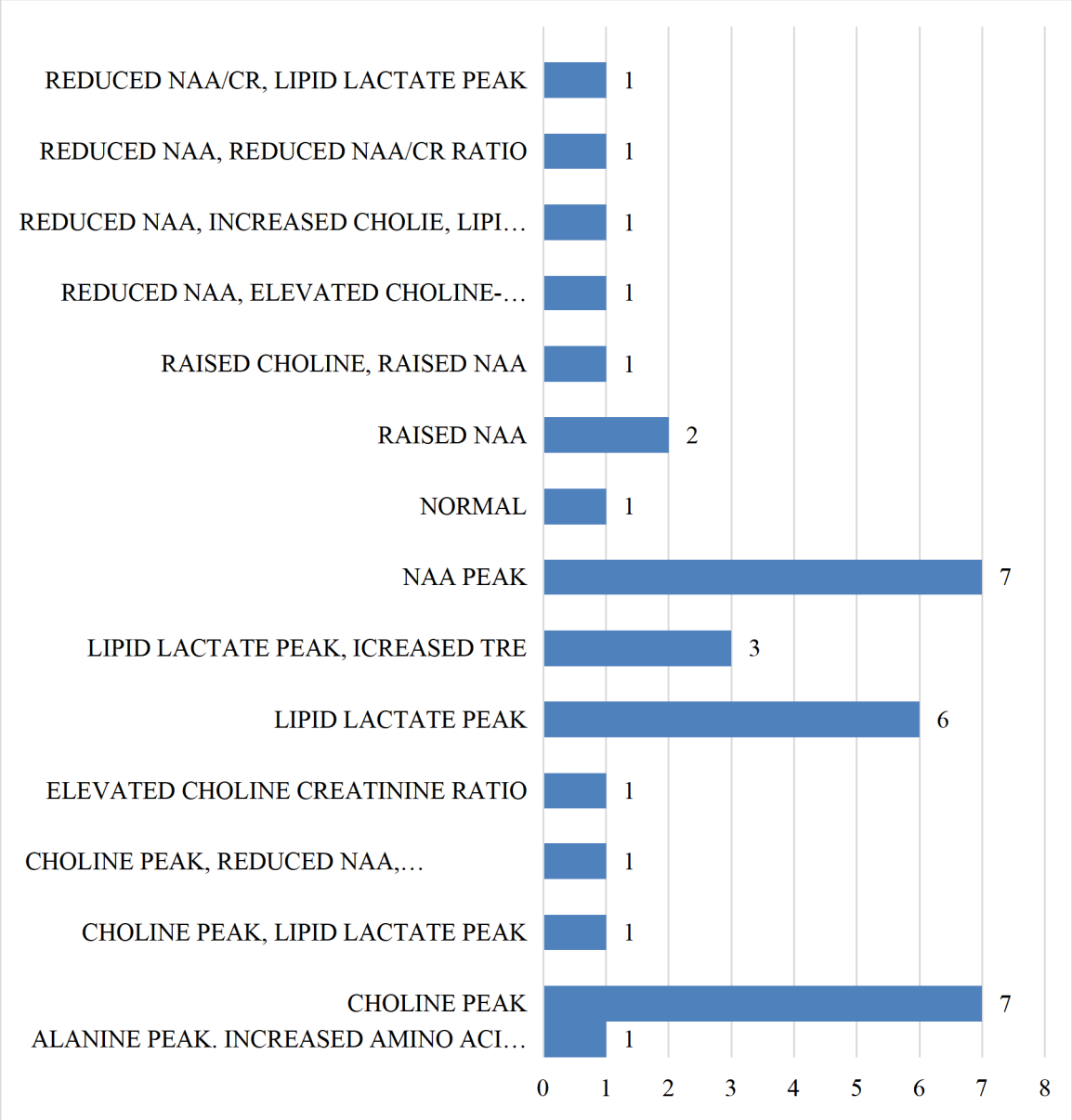


**Graph 7: Distribution of spectroscopy findings**

**Table 8: Distribution of diagnosis**

| Diagnosis | N | % |
|---|---|---|
| ASTROCYTOMA | 2 | 5.7% |
| BACTERIAL ABSCESS | 2 | 5.7% |
| GLIOMA | 2 | 5.7% |
| HIGH GRADE GLIOMA | 8 | 22.9% |
| HSV ENCEPHALITIS | 2 | 5.7% |
| METASTASIS (CA PROSTATE) | 1 | 2.9% |
| METASTASIS (CA BREAST) | 2 | 5.7% |
| METASTASIS (CA LUNG) | 2 | 5.7% |
| NCC | 2 | 5.7% |
| PILOCYTIC ASTROCYTOMA | 1 | 2.9% |
| PML (HIV) | 1 | 2.9% |
| TOXOPLASMOSIS | 2 | 5.7% |
| TUBERCULOMA | 8 | 22.9% |

8 (22.9%) each of the patients were diagnosed with tuberculoma and high-grade Glioma. There were the most common findings among the patients included in our study.

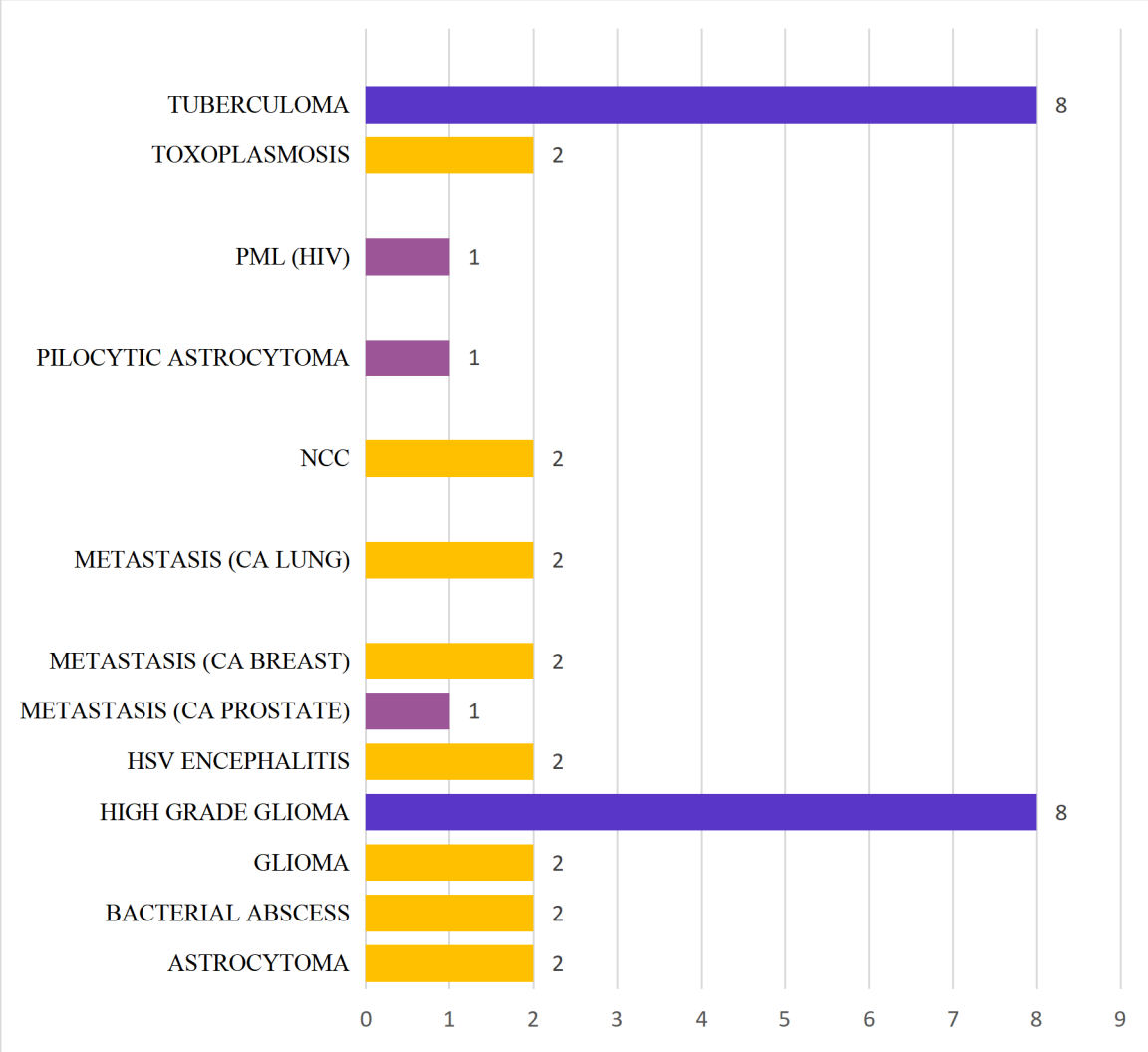


**Graph 8: Distribution of diagnosis**

**Table 9: Mean values of nCBFL and nCBFPE in various lesions**

| Group | Diagnosis (*N*) | Ncbfl Mean±SD | nCBFPE Mean±SD |
|---|---|---|---|
| Neoplastic | Primary lesions | 9.1 ± 5.2 | 2.9 ± 1.3 |
| | Metastases | 7.1 ± 2.13 | 0.9 ± 0.2 |
| Non-neoplastic | Tuberculoma | 1.75 ± 0.37 | 0.69 ± 0.31 |
| | NCC | 1.5 ± 0.42 | 1.2 ± 0.1 |
| | Toxoplasmosis | 1.9 ± 0.35 | 0.84 ± 0.11 |
| | Abscess | 1.52 ± 0.71 | 0.91 ± 0.1 |
| | Tumefactive demyelination | 0.59 ± 0.9 | 0.61 ± 0.57 |
| | Fungal granulomas | 1.3 ± 0.43 | 0.5± 0.9 |

p <0.01, neoplastic versus non-neoplastic

Above are the nCBFL and nCBFPE we observed in various lesions, based on which we found that the flow was significantly higher among the neoplastic lesions compared to non-neoplastic. Also, we found that it was significantly greater among primary neoplastic lesions than the metastatic lesions.

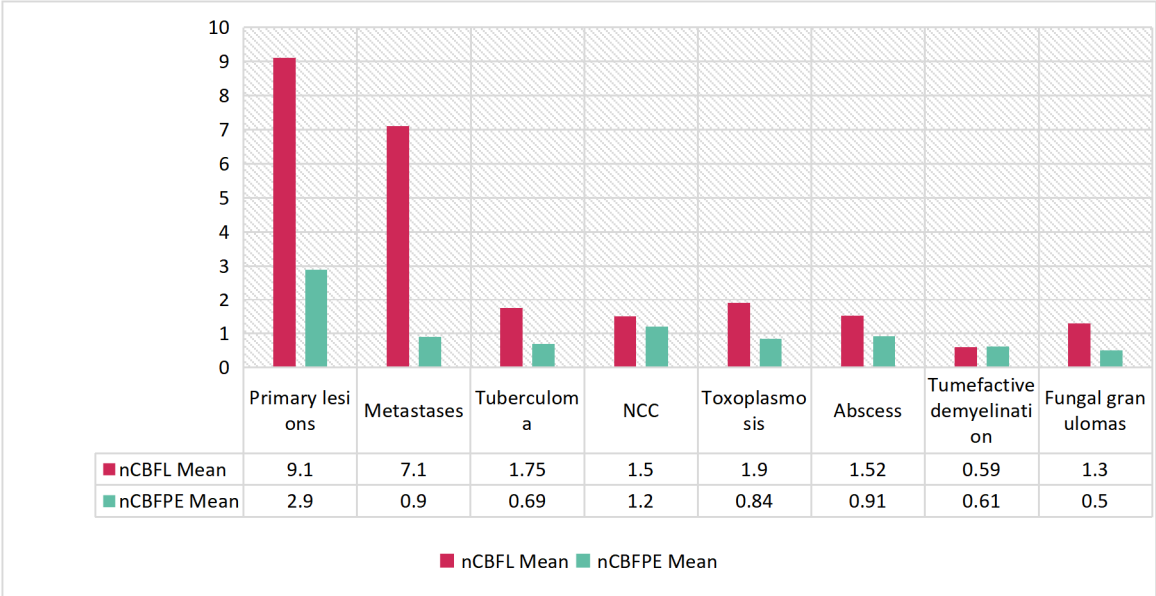


**Graph 9: Mean values of nCBFL and nCBFPE in various lesions**

**Table 10: Mean nCBFL and nCBFPE values among neoplastic and non-neoplastic group**

| ASL parameter | Neoplastic group | Non-neoplastic group | *p* value |
|---|---|---|---|
| nCBFL | 7.1 ± 3.9 | 2.1 ± 1.1 | <0.001 |
| nCBFPE | 1.9 ± 0.97 | 0.68 ± 0.32 | <0.001 |

In the table 10, we had observed that normalised cerebral blood for major lesions we had observed, here the table 11 provides us the average nCBFL and nCBFPE. According to the above table, the average values were significantly higher among neoplastic lesions than non- neoplastic lesions.

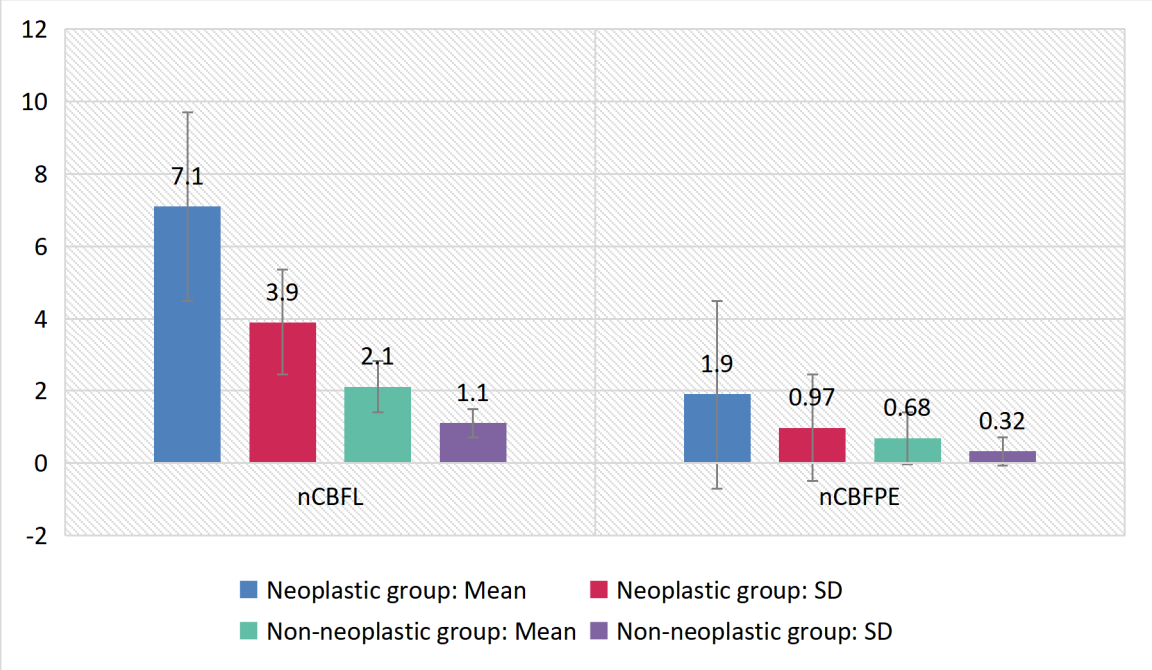


**Graph 10: Mean nCBFL and nCBFPE values among neoplastic and non-neoplastic group**

# DISCUSSION

As we had discussed in the previous section, contrast magnetic resonance imaging (MRI) had a well-established role in brain lesion evaluation by providing anatomical information. However, contrast MRI has a limited role in the quantitative and functional assessment of lesions in brain thus making it less reliable in differentiating tumors from tumor-like lesions.[68]

Contrast enhancement depicts the blood-brain barrier (BBB) impairment, so every lesion that shows contrast enhancement cannot be considered as a tumor and every glioma that does not take contrast might not be low-grade glioma and vice versa.[69]

Perfusion-weighted imaging (PWI) serves as a useful adjunct to conventional MRI and also overcomes the limitations of contrast MRI by estimating tumor neo angiogenesis, which helps in tumor grading, guiding stereotactic biopsy and surgical planning.

Dynamic susceptibility contrast (DSC) which is routinely used with PWI in the clinical diagnosis which uses an exogenous gadolinium contrast agent and provides the relative cerebral blood volume (rCBV) and relative cerebral blood flow (rCBF) parameters that correlate well with tumor grade and histology.[70]

Whereas the Arterial spin labeling (ASL) is another non-invasive PWI method providing the absolute quantification of CBF in the absence of exogenous contrast, which makes ASL a promising technique for studying perfusion in patients with allergies, renal failure, difficult intravenous access, repetitive follow-ups, pregnant women and children.

DSC is the most preferred tool for analysis over ASL in brain lesion evaluation because of routine contrast administration and the rapid data acquisition. However, in contrast-enhanced perfusion techniques, CBF quantification is affected by T1 and T2 effects of BBB disruption and susceptibility artifacts, which are comparatively lesser with ASL. Ata S et al shown a very strong correlation between ASL and DSC-MRI derived perfusion parameters for evaluation of brain tumors and support the possibility that ASL could be used as an alternative to DSC-MRI.[65,70]

**Cha S et al** and **Tourdias T et al** had explained that Gliomas are the most common primary brain tumors and sometimes differentiation from solitary enhancing cerebral metastases can be difficult on conventional MRI. Primary tumors have shown statistically significant higher perfusion in perilesional edema (PE) compared to metastases that have been ascribed to tumor infiltration along white matter tracts in glioma.[71,72]

We observed that 21 (60%) of the patients presented with headache followed by 34.3% (12) with seizures. 8 (22.9%), 6 (17.1%) and 5 (14.3%) had were presented with vomiting, altered sensorium and fever respectively. In the study by **Noguchi T et al** they observed that the patients presented with wide variation in the symptomatology. Initially with one or several overlapping neurological symptoms including abnormal behaviour in 6 patients, epilepsy among 6 patients, headache and impaired consciousness in 12, physical weakness among 5 patients, one each had loss of appetite, general fatigue, higher brain dysfunction respectively. Seven patients had an underlying illness, including acute myelocytic leukaemia treated by bone-marrow transplantation and so on. [67] We could observe that the symptomatology of the brain

disease varies with the chronicity of the disease as well as the underlying pathological conditions.

The above table illustrates the T1 morphology distributed among the study population. The incidence of hypo intense lesions were higher with the proportion of 48.6% (17) followed by 40% (14) with iso-intensend the rest 4 (11.4%) had found with hyperintense lesions.

We found that 82.9% (29) patients had observed with hyperintense lesions followed by 4 patients with isointense and the rest 2 patients had hypo intense lesions. With the above table we can see that diffusion restriction was found among 71.4% (25) of the study population and was absent among 28.6% (10) patients.

On MRI Imaging, all 36 these lesions appeared as hypo intense or isointense mass lesions on non-contrast MRI studies. After contrast administration, there was a ring- or a homogeneous disk-like enhancement within the region of hypointensity. The enhancing lesions are often of variable size and are usually surrounded by a varying amount of perifocal vasogenic edema. Typically, the ring-enhancing lesions were located at the junction of the gray and white matter, but in 5 cases they were present in the sub-cortical area, deep in the brain parenchyma or may even be superficial.

Several types of primary and secondary brain neoplasms, such as glioblastomas, low-grade gliomas, astrocytomas, lymphomas and brain metastases presented as multiple ring-enhancing lesions. 22.9 % were diagnosed as high-grade gliomas, 5.7% astrocytomas, 5.7 % as low grade glioblastomas, 5.7% as metastatic

lesions from carcinoma breast, 5.7% as metastasis from carcinomas from lung,2.9% as metastasis from carcinoma prostate and 2.9% as pilocystic astrocytoms.

Many non-neoplastic neurological disorders also presented with similar findings on MRI brain and contrast study, out of which 22.9 % were diagnosed as tuberculosis, 5.7 % as bacterial assesses, 5.7% as HIV encephalitis, 5.7 % as NCC, 5.7% as toxoplasmosis and 2.9% as PML.

**Schwartz *et al.***[68] reviewed 221 ring-enhancing lesions seen on MRI studies and reported that 40% were gliomas, 30% metastases, 8% abscesses and 6% demyelinating disease. In a majority of the cases, gliomas and metastatic lesions were single whereas abscesses and multiple sclerosis lesions were multiple. Metastatic deposits are often solid nodular lesions that may become ring-enhancing possibly because of central necrosis. In this study, multiple cortical or subcortical ring-enhancing lesions have also been encountered in patients with subacute bacterial endocarditis, indwelling catheters or other implanted devices such as cardiac valves.

Deep white matter ring-enhancing lesions, especially those with mass effect and surrounding vasogenic edema, are most often either primary brain tumors or abscesses.

The incidence of patients aged between 60 to 69 years were higher with the incidence of 11 (31.4%) followed by 7 (20%) aged between 50 to 59 years. Five (14.3%) each were aged between 20 to 29 years and 40 to 49 years. 4 (11.4%), 2 (5.7%) and 1 (2.9%) were aged between 30 to 39 years, 70 to 79 years and >79 years respectively. The average age of our study population was 63.8±9.4 years. We found 18 male and 17 female patients in our study. Similar study by **Noguchi T et al** who

had conducted ASL for infections, also had the patients with median age of 53.5 years.[67] Seems that elder age group are most commonly associated with brain lesions and often require MRI for the analysis.

As all the lesions, showed the same type of ring enhancement pattern on MRI Brain and contrast, ASL perfusion study was performed, which could classify the lesions based on the cerebral blood flow within the lesion and the perilesional edema by comparing it with the cerebral blood flow in the contralateral normal grey matter.

On conventional imaging, lymphoma and high-grade glioma cannot be differentiate, but MR perfusion shows the reduced rCBV values in lymphoma compared to malignant gliomas.

**Noguchi T et al** found that out of the 17 patients with non-purulent parenchymal involvement, high perfusion was detected in eight patients (47%).[67]

The study by **Nagouchi et al** on ASL-MRI revealed only one of the six patients (17%) with ventricular involvement of empyema due to unspecified bacterial infection. One each was found with PML due to HIV, pilocystic astrocytoma and metastatic lesion due to Ca prostate respectively.[67]

On analysing the cerebral blood flow (CBFL) and the perilesional flow (CBFPE) on ASL, we found that $9.1 \pm 5.2$ and $2.9 \pm 1.3$ were the nCBFL and nCBFPE in Primary lesions and Metastases respectively. nCBFL among the Tuberculoma, NCC, Toxoplasmosis, Abscess, Tumefactive demyelination and Fungal granulomas was $1.75 \pm 0.37$, $1.5 \pm 0.42$, $1.9 \pm 0.35$, $1.52 \pm 0.71$, $0.59 \pm 0.9$ and $1.3 \pm 0.43$ respectively. Whereas nCBFPE of the Tuberculoma, NCC, Toxoplasmosis, Abscess, Tumefactive demyelination and Fungal granulomas was $0.69 \pm 0.31$,

1.2 ± 0.1, 0.84 ± 0.11, 0.91 ± 0.1, 0.61 ± 0.57 and 0.5± 0.9. We found that the flow was significantly higher among the neoplastic lesions compared to non-neoplastic. Also, we found that it was significantly greater among primary neoplastic lesions than the metastatic lesions.

The average nCBFL for neoplastic and non-neoplastic lesions was 7.1 ± 3.9 and 2.1 ± 1.1 with significant p value of 0.01. nCBFPE for neoplastic and non-neoplastic lesions was 1.9 ± 0.97 and 0.68 ± 0.32, also had significant difference of p value of <0.01.

**Haller S et al** had been reported that in evaluation of tumors and a few on infections, most of these studies utilized the DSC perfusion technique and very few used ASL-MRI.[73] **Floriano VH et al** has found statistically significant higher rCBV values in neoplastic lesions than infectious lesions. **Floriano et al** found higher rCBV in neoplastic which was 4.28 ± 2.11 and in non-neoplastic lesions was found to be 0.63 ± 0.49 with a cutoff rCBV value of 1.3 with the sensitivity of 97.8% and specificity 92.6% for predicting malignancy. In our study we had not conducted the quantitative analysis of the CBF but we found significant difference in the CBF between WM and GM.[74] Hiremath et al has shown lower mean rCBV in TDL (2.11 ± 1.12) compared to mean rCBV in HGGs (3.77 ± 1.65).[75] Similar to which **Erdogan et al** also reported that even the capsular portion of abscesses had low flow compared to HGG and metastases.[76] Unlike to our observations, **Cha S et al** and **Blasel S et al** had found that TDL might also have high flow mimicking the HGG in few scenarios.[71,77]

**MR SPECTROSCOPY**

As ASL could only differentiate the ring enhancing lesions on the basis of cerebral blood flow into primary neoplasms and metastasis & into non neoplastic lesions, further added MR spectroscopy was needed to characterize the lesion and confirm the diagnosis.

NAA peak resonated at 2.0 ppm, which was decreased in any insult to brain including malignancies. Creatinine peak was observed at 3.02 ppm. It is the marker of aerobic energy metabolism; hence peak was constant. Peak was reduced in metastasis

Choline peak was observed at 3.2 ppm. Its peak reflected membrane turnover and hence was increased in neoplastic aetiologies.

Lactate peak was observed and was related to the final products of aerobic metabolism and hence its peak was observed in hypoxic ischemic tissues seen in infective aetiologies. Lipid peaks were observed at 0.9 and 1.3 ppm and was observed in necrosis seen in infective aetiologies as well as necrosis which occurred within tumours.

Increased choline and NAA ratio were seen in high grade gliomas and metastasis. Cho resonance is most prominent in regions with high neoplastic cellular density and is progressively lower in moderate and low-grade tumours. Similarly, decrease in NAA was reflective of impairment of normal functioning of neurons and axons with neoplastic tissue. Presence of creatine peaks has been taken as indication of low-grade tumours as below normal creatine levels have been considered to be the features of high-grade gliomas, and metastasis, thereby increasing the creatinine choline ratio.

The incidence of biochemical changes among the study samples were as below; Choline and NAA peak were the most common finding observed with the incidence of 7 (20%), followed by lipid lactate among 6 (17.1%) of the patients included in our study. 3 patients had found with lipid lactate peak, increased TRE, 2 were observed to be having peak NAA. 1 each were found with alkaline and amino acid peak, choline and lipid lactate peak, choline peak with elevated choline/ creat ratio and reduced NAA, Elevated choline: NAA, Raised choline and NAA, reduced NAA with elevated choline: creatinine, reduced NA with increased choline and lactate, reduced NAA as well as NAA:CR, reduced NAA/lipid lactate peak respectively. 22 patients determined to have meningeal involvement, high perfusion on ASL-MRI was seen in a high percentage of patients (77%) irrespective of pathogens.

**PRIMARY NEOPLASMS:**

Chon was higher in high-grade tumors compared with proved benign lesions stable lesions and demyelinating lesions High-grade tumors had a lower NAA than demyelinating lesions and stable lesions, and proved benign lesions and low-grade tumors. Low-grade tumors had 88.4% higher Cho than the proved benign lesions Cr did not show any significant differences among the examined groups of lesions. Considering all possible combinations of metabolite ratios, the best discriminant function to differentiate between the group of brain tumors (high-grade and low-grade) and the nonneoplastic lesions was found to include the ratios NAA/Cho, Cho, NAA, and NAA/Cr (presented in the decreasing magnitude of correlation with the discriminant function).

All cases of patients with NAA/Cho of 0.61 or less had abnormally elevated Cho; however, there was an overlap in Cho with non-neoplastic lesions (range, 0.38–2.32).

In our group of patients with ring enhancing brain lesions evaluated for suspected neoplasm, MRS and demonstrated a high rate of success in correctly classifying lesions originally diagnosed as tumors and nonneoplastic lesions on the basis of the ratios of NAA/Cho, Chonorm, NAAnorm, and NAA/Cr.

Choline and NAA peak were the most common finding observed with the incidence of 7 (20%), followed by lipid lactate among 6 (17.1%) of the patients included in our study.

Mean Cho/Cr and Cho/NAA ratios were 2.87±0.98 and 2.69±0.91 respectively. Mean Cho/Cr levels were recorded as 3.38±0.72 and 3.92±0.63 for high grade tumours and metastasis respectively.

The NAA/Cho range of 0.54 to 0.66 was considered as a cutoff in our study, with elevated levels of less than 0.6 were considered to be malignant.

Thus, in agreement with published data, our analyses confirmed that highly elevated Cho-containing compounds in conjunction with a decreased NAA resonance (resulting in decreased ratio of NAA/Cho) are parameters sensitively indicative of neoplastic tumoral growth and are helpful in differentiating tumors from other causes.

Elevated levels of Cho were detected in tumors compared with nonneoplastic lesions. Elevated signal intensity in Cho results from increased attenuation of proliferating tumoral cells, with Cho-containing compounds including membrane precursors and products of degradation

Tumoral levels of NAA, presumably originating from residual brain tissue within an infiltrating tumor were lower than in nonneoplastic lesions. Thus, in agreement with published data, our analyses confirmed that highly elevated Cho-containing compounds in conjunction with a decreased NAA resonance (resulting in decreased ratio of NAA/Cho) are parameters sensitively indicative of neoplastic tumoral growth and are helpful in differentiating tumors from other causes.

There was no significant difference in the level of Cr among the groups of different lesions. The levels of Cr in tumors in adults have been reported to be decreased or both increased and decreased.

In our study, high-grade tumors had a wider range of levels of Cr than low-grade tumors.

Some of the benign lesions may show decreased NAA levels, however they could be differentiated from malignant lesions as they did not show an elevated choline peak.

**METASTASIS:**

5 cases were metastasis (males=2; females=3). Multiple lesions were identified in all the five cases. All the cases showed high Cho /Cr and Cho /NAA levels. All 5 cases were hyperintense on T2 with 2 cases showing inversion on FLAIR suggestive of cystic metastasis. Primary was identified in three cases in breast, lung and prostrate. Thick, irregular type of ring enhancement was noted after contrast administration. Our findings were similar to the study conducted by **Vieth RG et al.**[78]

**TUBERCULOMA:**

On MRS, all the 8 tuberculoma lesions showed a lipid lactate peak, with 4 lesions showing reduced NAA peaks. The tubercular abscess also showed lipid lactate peak within it.

Lactate peak was identified at 1.3 ppm. Clear upwards peaks at 1.3 and 0.9 were defied as lipid peak,

**PYOGENIC ABSCESS:**

Among pyogenic abscesses 4 out of 7 cases showed an AA peak consisting of Acetate, Glycine and Alanine with 3 of the abscesses showing increased A/S ratio. 1 of the abscesses also showed lactate peak at the centre.

**D. Pal et al** performed a study on 194 patients which showed resonance of AAs with or without other metabolites in 80% of abscesses.[79] Our findings were similar to the study conducted by **TsuiEY et al.**[80]

**TOXOPLASMOSIS:**

2 cases of toxoplasmosis. On MRS, showed lipid lactate peak. Lactate peak was identified at 1.3 ppm. Clear upwards peaks at 1.3 and 0.9 were defied as lipid peak.

**NCC:**

2 cases of NCC showed a amino acid peak. (valine, leucine and isoleucine) Alanine peak was seen at 1.48 ppm, with increased acetate peak at 1.92 ppm and increased succinate peak at 2,4 ppm. A small aspartate peak at 2.6 ppm was also

observed in one case. Cho / Cr ratio was less than 1.1 in all NCC and more than 1.2 in all tuberculoma which is similar to the study performed by **Kumar et al** concluded that presence of lipid can be used for differentiating tuberculomas from both non-specific IG and NCC6.[81]

**PML:**

In HIV related PML lesions, all 4 cases showed reduced NAA with increased Choline. 2 of the lesions showed lactate peak while 2 cases showed increased myo inositol level within the lesion at 3.5 ppm

In a study by **L. Chang et al** they found patients with the highest survival had the highest level myoinositol.[82]

In the present study, 8 (22.9%) each of the patients were diagnosed with tuberculoma and high-grade Glioma. There were the most common findings among the patients included in our study. Two each were diagnosed with toxoplasmosis, NCC, Metastatic lesions from lungs, breast, Glioma, bacterial abscess, encephalitis and astrocytoma respectively.

# CONCLUSION

Multiple ring enhancing lesions are seen on MRI brain and contrast studies which can suggestive multiple diagnosis in lacing neoplastic aetiologies as well as being aetiologies.

Hence ASL is one of the reliable diagnostic tools for differentiating neoplastic and non-neoplastic lesions, and from differentiating neoplastic primary lesions from metastasis. Further added MR spectroscopy helps in conformation of the diagnosis.

A combination of the 3 help in getting closer to the accurate diagnosis thereby reducing the need off biopsies, helping to start early treatment.

# SUMMARY


- The present study was conducted on 36 patients, suspected cases of brain lesion to detect Ring enhancing lesions on MRI Scan and further use advanced MR techniques like Arterial Spin labeling (ASL) and MR Spectroscopy to differentiate them into Benign and Malignant lesions (High grade versus low grade, primary versus metastatic)
- To further characterize these rings enhancing lesion into neuro infections, abscess, demyelinating lesions and other lesions.
- Average age of our study population was 63.8±9.4 years.
- There was no significant correlation observed between the demographic details and the incidence of lesions either on MRS or on ASL
- Headache in 60% of the population was the common symptoms.
- The incidence of hypodense lesions were higher with the proportion of 48.6% (17) on T1 morphology.
- 82.9% (29) patients had observed with hyperdense lesions on T2 morphology.
- Diffusion was restricted among 71.4% of the patients.
- Choline and NAA peak were the most common finding observed with the incidence of 7 (20%), followed by lipid lactate among 6 (17.1%) of the patients included in our study.
- 8 (22.9%) each of the patients were diagnosed with tuberculoma and high-grade Glioma were the most common findings among the patients included in our study.

- We found that the flow was significantly higher among the neoplastic lesions compared to non-neoplastic. Also, we found that it was significantly greater among primary neoplastic lesions than the metastatic lesions.
- Average nCBFL and nCBFPE were significantly higher among neoplastic lesions than non- neoplastic lesions.

# BIBLIOGRAPHY

1. Shetty G, Avabratha KS, Rai BS. Ring-enhancing lesions in the brain: a diagnostic dilemma. Iran J Child Neurol. 2014 Summer;8(3):61-4.
2. Horská A, Barker PB. Imaging of brain tumors: MR spectroscopy and metabolic imaging. Neuroimaging Clin N Am. 2010 Aug;20(3):293-310.
3. Seth R, Kalra V, Sharma U, Jagannathan N. Magnetic resonance spectroscopy in ring enhancing lesions. *Indian pediatrics.* 2010;47(9):803–4. Epub 2010/11/05.
4. Rudresh K MKM, Karthik , Sebastin J. Clinical and Aetiological Profile of Ring-enhancing Lesions on CT Brain. *Journal of Indian Academy of Clinical Medicine.* 2008;9(2):100–2.
5. Li Y, Park I, Nelson SJ. Imaging tumor metabolism using in vivo magnetic resonance spectroscopy. Cancer J. 2015 Mar-Apr;21(2):123-8.
6. McKnight TR, Noworolski SM, Vigneron DB, et al. An automated technique for the quantitative assessment of 3D-MRSI data from patients with glioma. *J Magn Reson Imaging.* 2001;13:167–177.
7. Park I, Chen AP, Zierhut ML, et al. Implementation of 3 T lactate-edited 3D 1H MR spectroscopic imaging with flyback echo-planar readout for gliomas patients. *Ann Biomed Eng.* 2011;39:193–204.
8. Detre JA, Rao H, Wang DJ, Chen YF, Wang Z. Applications of arterial spin labeled MRI in the brain. *J Magn Reson Imaging* 2012; 35: 1026–1037.
9. Shampo MA, Kyle RA, Steensma DP. Richard Ernst--Nobel Prize for nuclear magnetic resonance spectroscopy. Mayo Clin Proc. 2012 Dec;87(12):e109.
10. Berger A. Magnetic resonance imaging. BMJ. 2002 Jan 5;324(7328):35.

11. Grover VP, Tognarelli JM, Crossey MM, Cox IJ, Taylor-Robinson SD, McPhail MJ. Magnetic Resonance Imaging: Principles and Techniques: Lessons for Clinicians. J Clin Exp Hepatol. 2015 Sep;5(3):246-55.

12. Westbrook C., Roth C.K., Talbot J. 4th edition. John Wiley & Sons, Inc.; London: 2011. MRI in Practice.

13. Stadnik T.W., Chaskis C., Michotte A. Diffuion-weighted MR imaging of intracerebral masses: comparison with conventional MR imaging and histologic findings. *AJNR Am J Neuroradiol.* 2001;22(5):969–976.

14. Chan KY, Siu JCW. Magnetic Resonance Imaging Features of Cerebral Ring-Enhancing Lesions with Different Aetiologies: a Pictorial Essay. Hong Kong J Radiol. 2021;24(1):62-74

15. Parihar A, Tomar V, Ojha BK, Husain N, Gupta RK. Magnetic resonance imaging findings in a patient with isolated histoplasma brain abscess. *Arch Neurol*. 2011;68(4):534–535.

16. Cortese I, Nath A. Case 11: a young woman with ring-enhancing brain lesions. Med Gen Med. 2006 Jan 5;8(1):3.

17. Tognarelli JM, Dawood M, Shariff MI, Grover VP, Crossey MM, Cox IJ, Taylor-Robinson SD, McPhail MJ. Magnetic Resonance Spectroscopy: Principles and Techniques: Lessons for Clinicians. J Clin Exp Hepatol. 2015 Dec;5(4):320-8.

18. Verma A, Kumar I, Verma N, Aggarwal P, Ojha R. Magnetic resonance spectroscopy - Revisiting the biochemical and molecular milieu of brain tumors. BBA Clin. 2016 Apr 12;5:170-8.

19. Griffin J.L., Shockcor J.P. Metabolic profiles of cancer cells. *Nat. Rev. Cancer*. 2004;4:551–561.

20. Zhu H, Barker PB. MR spectroscopy and spectroscopic imaging of the brain. Methods Mol Biol. 2011;711:203-26.

21. Govindaraju V, Young K, Maudsley AA. Proton NMR chemical shifts and coupling constants for brain metabolites. *NMR Biomed.* 2000;13(3):129–153

22. Barker P, Breiter S, Soher B, Chatham J, Forder J, Samphilipo M, Magee C, Anderson J. Quantitative proton spectroscopy of canine brain: In vivo and in vitro correlations. *Magn Reson Med.* 1994;32:157–163

23. Lunsing RJ, Strating K, de Koning TJ, Sijens PE. Diagnostic value of MRS-quantified brain tissue lactate level in identifying children with mitochondrial disorders. Eur Radiol. 2017 Mar;27(3):976-984.

24. Krishnamoorthy T, Radhakrishnan VV, Thomas B, Jeyadevan ER, Menon G, Nair S. Alanine peak in central neurocytomas on proton MR spectroscopy. Neuroradiology. 2007 Jul;49(7):551-4.

25. Lai P.H., Li K.T., Hsu S.S. Pyogenic brain abscess: findings from in vivo 1.5-T and 11.7-T in vitro proton MR spectroscopy. *Am. J. Neuroradiol.* 2005;26:279–288.

26. Pillai J., Kwock L., Horsk A. Brain Magnetic Resonance Spectroscopy. In: Haaga J.R., Lanzieri C.F., Gilkeson R.C., editors. *CT and MR Imaging of the Whole Body.* Vol. 1. 2003. pp. 371–395.

27. Dezortova M, Jiru F, Petrasek J, Malinova V, Zeman J, Jirsa M, Hajek M. 1H MR spectroscopy as a diagnostic tool for cerebral creatine deficiency. MAGMA. 2008 Sep;21(5):327-32.

28. American College of Radiology, American Society of Neuroradiology Society of Pediatric Radiology: ACR-ASNR-SPR practice guideline for the performance and interpretation of magnetic resonance spectroscopy of the

central nervous system, revised. 2013. http://www.acr.org/~/media/ ACR/Documents/PGTS/guidelines/MR_Spectroscopy.pdf

29. Sener RN. Proton MR spectroscopy demonstration of taurine peaks in megalencephalic leukoencephalopathy with cysts. Comput Med Imaging Graph. 2003;27(1):23-6.
30. Mullins M.E. MR spectroscopy: truly molecular imaging; past,present and future. *Neuroimaging Clin. N. Am.* 2006;16(4):605–618
31. Law M., Yang S. Glioma grading: sensitivity, specificity, and predictive values of perfusion MR imaging and proton MR spectroscopic imaging compared with conventional MR imaging. *AJNR Am. J. Neuroradiol.* 2003;24(10):1989–1998.
32. Kousi E., Tsougos I., Kapsalaki E. *Novel Frontiers of Advanced Neuroimaging.* InTech; 2013. Proton Magnetic Resonance Spectroscopy of the Central Nervous System; pp. 19–50
33. Petcharunpaisan S, Ramalho J, Castillo M. Arterial spin labeling in neuroimaging. World J Radiol. 2010 Oct 28;2(10):384-98.
34. Petersen ET, Lim T, Golay X. Model-free arterial spin labeling quantification approach for perfusion MRI. Magn Reson Med. 2006;**55**:219–232.
35. Deibler AR, Pollock JM, Kraft RA, Tan H, Burdette JH, Maldjian JA. Arterial spin-labeling in routine clinical practice, part 1: technique and artifacts. AJNR Am J Neuroradiol. 2008;**29**:1228–1234.
36. Pollock JM, Tan H, Kraft RA, Whitlow CT, Burdette JH, Maldjian JA. Arterial spin-labeled MR perfusion imaging: clinical applications. Magn Reson Imaging Clin N Am. 2009;**17**:315–338.

37. Detre JA, Wang J, Wang Z, Rao H. Arterial spin-labeled perfusion MRI in basic and clinical neuroscience. Curr Opin Neurol. 2009;**22**:348–355.

38. Wolf RL, Detre JA. Clinical neuroimaging using arterial spin-labeled perfusion magnetic resonance imaging. Neurotherapeutics. 2007;**4**:346–359

39. Golay X, Petersen ET. Arterial spin labeling: benefits and pitfalls of high magnetic field. Neuroimaging Clin N Am. 2006;**16**:259–268

40. MacIntosh BJ, Filippini N, Chappell MA, Woolrich MW, Mackay CE, Jezzard P. Assessment of arterial arrival times derived from multiple inversion time pulsed arterial spin labeling MRI. Magn Reson Med. 2010;**63**:641–647.

41. Liu TT, Brown GG. Measurement of cerebral perfusion with arterial spin labeling: Part 1. Methods. J Int Neuropsychol Soc. 2007;**13**:517–525.

42. Barbier EL, Lamalle L, Décorps M. Methodology of brain perfusion imaging. J Magn Reson Imaging. 2001;**13**:496–520.

43. Wong EC. Quantifying CBF with pulsed ASL: technical and pulse sequence factors. J Magn Reson Imaging. 2005;**22**:727–731.

44. Wu WC, Fernández-Seara M, Detre JA, Wehrli FW, Wang J. A theoretical and experimental investigation of the tagging efficiency of pseudocontinuous arterial spin labeling. Magn Reson Med. 2007;**58**:1020–1027.

45. Hu Y, Liu R, Gao F. Arterial Spin Labeling Magnetic Resonance Imaging in Healthy Adults: Mathematical Model Fitting to Assess Age-Related Perfusion Pattern. Korean J Radiol. 2021 Jul;22(7):1194-1202.

46. Wang J, Licht DJ, Jahng GH, Liu CS, Rubin JT, Haselgrove J, Zimmerman RA, Detre JA. Pediatric perfusion imaging using pulsed arterial spin labeling. J Magn Reson Imaging. 2003;**18**:404–413.

47. Golay X, Hendrikse J, Lim TC. Perfusion imaging using arterial spin labeling. Top Magn Reson Imaging. 2004;**15**:10–27

48. Ding B, Ling HW, Zhang Y, Huang J, Zhang H, Wang T, Yan FH. Pattern of cerebral hyperperfusion in Alzheimer's disease and amnestic mild cognitive impairment using voxel-based analysis of 3D arterial spin-labeling imaging: initial experience. Clin Interv Aging. 2014 Mar 26;9:493-500.

49. van Gelderen P, de Zwart JA, Duyn JH. Pittfalls of MRI measurement of white matter perfusion based on arterial spin labeling. Magn Reson Med. 2008;**59**:788–795.

50. van Osch MJ, Teeuwisse WM, van Walderveen MA, Hendrikse J, Kies DA, van Buchem MA. Can arterial spin labeling detect white matter perfusion signal? Magn Reson Med. 2009;**62**:165–173.

51. Chen J, Licht DJ, Smith SE, Agner SC, Mason S, Wang S, Silvestre DW, Detre JA, Zimmerman RA, Ichord RN, et al. Arterial spin labeling perfusion MRI in pediatric arterial ischemic stroke: initial experiences. J Magn Reson Imaging. 2009;**29**:282–290.

52. Zaharchuk G. Arterial spin label imaging of acute ischemic stroke and transient ischemic attack. Neuroimaging Clin N Am. 2011 May;21(2):285-301

53. Wolf RL, Wang J, Detre JA, Zager EL, Hurst RW. Arteriovenous shunt visualization in arteriovenous malformations with arterial spin-labeling MR imaging. AJNR Am J Neuroradiol. 2008;**29**:681–687

54. Boulouis G, Dangouloff-Ros V, Boccara O, Garabedian N, Soupre V, Picard A et al. Arterial Spin-Labeling to Discriminate Pediatric Cervicofacial Soft-Tissue Vascular Anomalies. AJNR Am J Neuroradiol. 2017 Mar;38(3): 633-638.

55. Wolk DA, Detre JA. Arterial spin labeling MRI: an emerging biomarker for Alzheimer's disease and other neurodegenerative conditions. Curr Opin Neurol. 2012 Aug;25(4):421-8.

56. Musiek ES, Chen Y, Korczykowski M, Saboury B, Martinez PM, Reddin JS, Alavi A et al Direct comparison of fluorodeoxyglucose positron emission tomography and arterial spin labeling magnetic resonance imaging in Alzheimer's disease. Alzheimers Dement. 2012 Jan;8(1):51-9.

57. Wolk DA, Detre JA. Arterial spin labeling MRI: an emerging biomarker for Alzheimer's disease and other neurodegenerative conditions. Curr Opin Neurol. 2012 Aug;25(4):421-8

58. Yoo RE, Yun TJ, Yoon BW, Lee SK, Lee ST et al. Identification of cerebral perfusion using arterial spin labeling in patients with seizures in acute settings. PLoS One. 2017 Mar 14;12(3):e0173538.

59. Bansal V, Kumar S, Sharma S, Sharma S, Sood RG. Usefulness of Pulsed Arterial Spin Labeling Magnetic Resonance Imaging in New-onset Seizure Patients and Its Comparison with Dynamic Susceptibility Contrast Magnetic Resonance Imaging. J Neurosci Rural Pract. 2017 Oct-Dec;8(4):569-574

60. Fu M, Han F, Feng C, Chen T, Feng X. Based on arterial spin labeling helps to differentiate high-grade gliomas from brain solitary metastasis: A systematic review and meta-analysis. Medicine (Baltimore). 2019 May;98(19):e15580.

61. Delgado AF, De Luca F, Hanagandi P, van Westen D, Delgado AF. Arterial Spin-Labeling in Children with Brain Tumor: A Meta-Analysis. AJNR Am J Neuroradiol. 2018 Aug;39(8):1536-1542.

62. Alsaedi A, Doniselli F, Jäger HR, Panovska-Griffiths J, Rojas-Garcia A, Golay X, Bisdas S. The value of arterial spin labelling in adults glioma grading:

systematic review and meta-analysis. Oncotarget. 2019 Feb 22;10(16):1589-1601

63. Patil YP, Patel CR, Kuber RS, Sekhon RK. Characteristics of Ring enhancing lesions in brain in correlation with MRI and MR spectroscopy. Int J Health Clin Res. 2021;4(1):120-127
64. Seth R, Kalra V, Sharma U, Jagannathan N. Magnetic resonance spectroscopy in ring enhancing lesions. Indian Pediatr. 2010 Sep;47(9):803-4.
65. Soni N, Srindharan K, Kumar S, Mishra P, Bathla G, Kalita J, Behari S. Arterial spin labeling perfusion: Prospective MR imaging in differentiating neoplastic from non-neoplastic intra-axial brain lesions. Neuroradiol J. 2018 Dec;31(6):544-553.
66. Chawla S, Wang S, Wolf RL, Woo JH, Wang J, O'Rourke DM, Judy KD, Grady MS, Melhem ER, Poptani H. Arterial spin-labeling and MR spectroscopy in the differentiation of gliomas. AJNR Am J Neuroradiol. 2007 Oct;28(9):1683-9.
67. Noguchi T, Yakushiji Y, Nishihara M, Togao O, Yamashita K, Kikuchi K, Matsuo M, Azama S, Irie H. Arterial Spin-labeling in Central Nervous System Infection. Magn Reson Med Sci. 2016 Oct 11;15(4):386-394.
68. Omuro AM, Leite CC, Mokhtari K, et al. Pitfalls in the diagnosis of brain tumours. *Lancet Neurol* 2006; 5: 937–948.
69. Law M, Yang S, Babb JS. Comparison of cerebral blood volume and vascular permeability from dynamic susceptibility contrast-enhanced perfusion MR imaging with glioma grade. *AJNR Am J Neuroradiol* 2004; 25: 746–755.

70. Grade M, Hernandez Tamames JA, Pizzini FB. A neuroradiologist's guide to arterial spin labeling MRI in clinical practice. *Neuroradiology* 2015; 57: 1181–1202.

71. Cha S, Lupo JM, Chen MH, et al. Differentiation of glioblastoma multiforme and single brain metastasis by peak height and percentage of signal intensity recovery derived from dynamic susceptibility-weighted contrast-enhanced perfusion MR imaging. *AJNR Am J Neuroradiol* 2007; 28: 1078–1084

72. Tourdias T, Rodrigo S, Oppenheim C, et al. Pulsed arterial spin labeling applications in brain tumors: Practical review. *J Neuroradiol* 2008; 35: 79–89.

73. Haller S, Zaharchuk G, Thomas DL. Arterial spin labeling perfusion of the brain: Emerging clinical applications. *Radiology* 2016; 281: 337–356.

74. Floriano VH, Torres US, Spotti AR, et al. The role of dynamic susceptibility contrast-enhanced perfusion MR imaging in differentiating between infectious and neoplastic focal brain lesions: Results from a cohort of 100 consecutive patients. *PLoS One* 2013; 8: e81509.

75. Hiremath SB, Muraleedharan A, Kumar S, et al. Combining diffusion tensor metrics and DSC perfusion imaging: Can it improve the diagnostic accuracy in differentiating tumefactive demyelination from high-grade glioma? *AJNR Am J Neuroradiol* 2017; 38: 685–690.

76. Hakyemez B, Erdogan C, Bolca N, Yildirim N, Gokalp G, Parlak M. Evaluation of different cerebral mass lesions by perfusion-weighted MR imaging. Journal of Magnetic Resonance Imaging: An Official Journal of the International Society for Magnetic Resonance in Medicine. 2006 Oct;24(4):817-24.

77. Blasel S, Franz K, Ackermann H, Weidauer S, Zanella F, Hattingen E. Stripe-like increase of rCBV beyond the visible border of glioblastomas: site of tumor infiltration growing after neurosurgery. *Journal of Neuro-Oncology*. 2011;103(3):575–584.

78. Kamada K, Möller M, Saguer M, Ganslandt O, Kaltenhäuser M, Kober H, Vieth J. A combined study of tumor-related brain lesions using MEG and proton MR spectroscopic imaging. Journal of the neurological sciences. 2001 May 1;186(1-2):13-21.

79. D. Pal , A. Bhattacharyya ,M. Husain ,K.N. Prasad ,C.M. Pandey ,R.K. Gupta In Vivo Proton MR Spectroscopy Evaluation of Pyogenic Brain Abscesses: A Report of 194 Cases AJNR Am J Neuroradiol Feb 2010 31:360– 66

80. Tsui EY, Chan JH, Cheung YK, Lai KF, Fong D, Ng SH Evaluation of cerebral abscesses by diffusion-weighted MR imaging and MR spectroscopy; Comput Med Imaging Graph. 2002Sep-Oct;26(5):347-51.

81. Kumar A, Kaushik S, Tripathi RP, Kaur P, Khushu S. Role of in vivo proton MR spectroscopy in the evaluation of adult brain lesions: Ourpreliminary experience. Neurol India 2003; 51: 474-478.

82. Kee-Hyun Chang, In Chan Song, Sung Hyun Kim, Moon Hee Han et al In Vivo Differentiation of Aerobic Brain Abscesses and Necrotic Glioblastomas Multiforme Using Proton MR Spectroscopic Imaging AJNR Am J Neuroradiol29:1511–18

# ANNEXURE – I – INFORMED CONSENT

**TITLE OF THE STUDY: "EVALUATION OF RING ENHANCING LESIONS IN BRAIN IN CORELATION WITH ARTERIAL SPIN LABELING AND MR SPECTROSCOPY'**

**INVESTIGATOR: Dr.**

**GUIDE : DR.**

**INTRODUCTION AND PURPOSE:**

The purpose of this study is to detect all ring enhancing lesions on conventional MRI Imaging and use superior advanced techniques like ASL sequencing and MR spectroscopy for better differentiation of brain lesions,which will help in better detection,staging,treatment and prognosis of the disease.

**PROCEDURE:**

The purpose of the study will be explained and written informed consent will be obtained from all participants.

The subjects will be selected based on inclusion and exclusion criteria.

Study will be conducted over a period of one year. Once the patient signs the informed consent, history and examination will be recorded as per proforma.

They will be asked to changed into an examination gown and will be asked to lie down still in supine position on the MRI table. They will also be told about the humming sound which they will hear during the scan which is harmless..

I request you to kindly participate in the study titled study**"EVALUATION OF RING ENHANCING LESIONS IN BRAIN IN CORELATION WITH ARTERIAL SPIN LABELING AND MR SPECTROSCOPY"** at Dr. Prabhakar Kore Hospital and Medical Research Centre, Belagavi is being conducted by

Post graduate in Radio diagnosis at J.N. Medical College, Belagavi, Karnataka, under the guidance of

Dept. of Radio-diagnosis, J. N. Medical College, Belagavi.

We request you to participate in this study as you are eligible to be included. During the study, you will be asked questions regarding your present and past medical history and you will be required to answer to the best of your knowledge. You will also be clinically examined as per the protocol drawn.

If you agree to participate in the study, please furnish the details pertaining to the study.

**BENEFITS:**

- No use of surgical equipment /risk associated with it.

**COMPLICATIONS:**

- No risks or complications involved

**ALTERNATIVES:**

If you are not willing to take part in the study, your treatment or any other further investigations the patient wants to undergo, in future, in KLE will not be affected by your decision.

| | | |
|---|---|---|
| 1. | | |
| 2. | | |
| 3. | | |

HISTORY OF PRESENTING ILLNESS:

| | | |
|---|---|---|
| 1. | | |
| 2. | | |
| 3. | | |

PAST HISTORY

| | | |
|---|---|---|
| 1. | | |
| 2. | | |
| 3. | | |

CLINICAL EXAMINATION:

CNS

MRI FINDINGS:

ASL SEQUENCING FINDINGS

change my willingness to continue to take part. If you choose not to take part in the study, you will receive the standard treatment for patients with your condition.

**COSTS:**

NIL (The study is to be conducted on the participants who are advised CT or MRI with ASL Perfusion and MR Spectroscopy as an investigation by the referring consultant and the participants will bear the charges for it.)

**Payment for Participation:** No incentive will be paid to you for participating in this study.

**COMPENSATION:**

In the event that you become injured as a result of taking part in this study, treatment whatever available at KLE Charitable hospital, Belagavi, will be offered to you. No reimbursement, compensation or free medical care is given.

**CONFIDENTIALITY:**

All information collected about you during the course of the study will be kept confidential to the extent permitted by the law. The code numbers will identify you in this research record. Information from this study may be published but your identity will be kept confidential in any publication/ presentation.

**QUESTION:**

If you have any enquiries in the future or in case of research related injury illness, you may contact following persons:

DR.HARSHA HEGDE.

CHAIRPERSON,
JNMC, IEC & SCIENTIST D,
ICMR, NATIONAL INSTITUE
OF TRADITIONAL MEDICINE,
BELAGAVI

Ph. No: 0831-2473777,Ext.
1529

# ANNEXURE – II - PROFORMA

**KAHER**

**J. N. MEDICAL COLLEGE, BELAGAVI.**

**DEPARTMENT OF RADIODIAGNOSIS**

**TITLE:"EVALUATION OF RING ENHANCING LESIONS IN BRAIN IN CORRELATION WITH MR SPECTROSCOPY AND ARTERIAL SPIN LABELING "**

**RESEARCH INVESTIGATOR :**

**GUIDE :**

**PROFORMA FOR DATA COLLECTION**

**DATE OF INTERVIEW : _____**

**NAME OF THE PATIENT :_____**

**AGE (in years) :_____ SEX: OP/IP NO _____**

**MOBILENUMBER :_____**

**ADDRESS : House No_____ Galli _____ Ward/ Village _____**

**City _____ District _____ PIN CODE : _____**

**MRI/CT NUMBER: _____**

**MRI SPECTROSCOPY FINDINGS**

**FINAL DIAGNOSIS:**

## ANNEXURE - III - MASTER CHART

| SLNO | NAME | AGE | SEX | SYMPTOMS | T1 MORPHOLOGY | T2 MORPHOLOGY | DIFFUSION RESTRICTION | ASL rCBF-LESION | ASL rCBF - PPERILESIONAL EDEMA | RATIO OF ASL rCBF LESION-CONTRALATERAL WHITE MATTER | RATIO OF ASL rCBF PE-CONTRALATERAL WHITE MATTER | CBF IN NORMAL CONTRALATERAL WHITE MATTER | SPECTROSCOPY | DIAGNOSIS |
|---|---|---|---|---|---|---|---|---|---|---|---|---|---|---|
| 1 | VILAS BHADANGE | 60 | M | ALTERED SENSORIUM | Hypointense | Hyperintense | + | 670 | 80 | 6 70./100 | 80./100 | 100 | CHOLINE PEAK | METASTASIS (CA LUNG) |
| 2 | RAMASIDDA MALAGI | 51 | M | SEIZURES, HEADACHE | Hypointense | Hyperintense | + | 790 | 31 | 7 90. /101 | 31./101 | 101 | CHOLINE PEAK, REDUCED NAA, ELEVATED CHOLINE CREATININE RATIO | ASTROCYTOMA |
| 3 | VITHAL BHOJAN | 65 | M | SEIZURES, ALTERED SENSORIUM | Hypointense | Hyperintense | + | 810 | 36 | 7 13. /112 | 36./112 | 112 | NAA PEAK | HIGH GRADE GLIOMA |
| 4 | MAHADEV VADDIN | 65 | M | HEADACHE, SEIZURES | Isointense | Isointense | + | 860 | 39 | 860. / 100 | 39./100 | 100 | NAA PEAK | HIGH GRADE GLIOMA |
| 5 | KALPANA HUDDAR | 47 | F | ALTERED SENSORIUM | Isointense | Hyperintense | + | 700 | 9 | 700./ 98 | 9./98 | 98 | CHOLINE PEAK | METASTASIS (CA BREAST) |
| 6 | VIMAL NIKAM | 64 | F | HEADACHE, VOMITTING | Hypointense | Isointense | + | 680 | 8 | 680./104 | 8./104 | 104 | CHOLINE PEAK | METASTASIS (CA BREAST) |
| 7 | MAYADEVI MADAR | 52 | F | HEADACHE, FEVER, MOTOR WEAKNESS | Isointense | Hyperintense | + | 810 | 33 | 810./110 | 33./110 | 110 | ELEVATED CHOLINE CREATININE RATIO | ASTROCYTOMA |
| 8 | ASMITA B | 22 | F | HEADACHE, SEIZURES | Hypointense | Hyperintense | + | 840 | 32 | 840./125 | 32./125 | 125 | REDUCED NAA, ELEVATED CHOLINE-CREATININE RATIO | PILOCYTIC ASTROCYTOMA |
| 9 | AHMED KAZI | 72 | M | ALTERED SENSORIUM | Hypointense | Hyperintense | + | 730 | 9 | 730./100 | 7./100 | 100 | CHOLINE PEAK | METASTASIS (CA LUNG) |
| 10 | IBADULLA HUDALI | 52 | M | ALTERED SENSORIUM | Isointense | Isointense | + | 890 | 31 | 890./99 | 31./99 | 99 |  | HIGH GRADE GLIOMA |
| 11 | INDUBAI GURAV | 60 | F | HEADACHE, VOMITTING | Hypointense | Hyperintense | _ | 160 | 8 | 160./98 | 8./98 | 98 | LIPID LACTATE PEAK,REDUCED NAA AND CHOLINE PEAK | TUBERCULOMA |
| 12 | BASAPPA PATIL | 49 | M | SEIZURES, FEVER | Isointense | Hyperintense | + | 170 | 7 | 170./97 | 7./97 | 97 | ALANINE PEAK. INCREASED AMINO ACID PEAK | BRAIN ABSCESS |
| 13 | AKKAVVA M | 80 | F | ALTERED SENSORIUM | Hypointense | Hyperintense | + | 860 | 31 | 860./98 | 31./98 | 98 | NAA PEAK | HIGH GRADE GLIOMA |
| 14 | VISHNU KANKEKAR | 71 | M | SLURRED SPEECH, SEIZURES | Hypointense | Hyperintense | + | 890 | 35 | 890./100 | 35./100 | 100 | NAA PEAK | HIGH GRADE GLIOMA |
| 15 | ABDUL GIRUKAR | 61 | M | FEVER, SEIZURES | Hyperintense | Hypointense | _ | 190 | 8 | 190./102 | 8./102 | 102 | LIPID LACTATE PEAK | BACTERIAL ABSCESS |
| 16 | ANANTMURTHI GUDI | 29 | M | HEADACHE, VOMITTING | Isointense | Hypointense | - | 180 | 6 | 180./112 | 6./112 | 112 | REDUCED NAA/CR, LIPID LACTATE PEAK | TUBERCULOMA |
| 17 | CHANDRAKANT B | 60 | M | HEADACHE, SEIZURES | Hypointense | Hyperintense | + | 150 | 5 | 150./100 | 5./100 | 100 | LIPID LACTATE PEAK | TUBERCULOMA |
| 18 | DHANAVVA | 60 | F | FEVER, SEIZURES | Hypointense | Hyperintense | + | 140 | 6 | 140./100 | 6./100 | 100 | REDUCED NAA, REDUCED NAA/CR RATIO | HSV ENCEPHALITIS |
| 19 | JAYAWANT PATIL | 51 | M | HEADACHE, SEIZURES | Hypointense | Hyperintense | _ | 180 | 7 | 180./94 | 7./94 | 94 | LIPID LACTATE PEAK, REDUCED NAA | TOXOPLASMOSIS |
| 20 | JINAPPA K | 56 | M | HEADACHE, SEIZURES | Isointense | Hyperintense | _ | 130 | 8 | 130./98 | 8./98 | 98 | REDUCED NAA, INCREASED CHOLIE, LIPID LACTATE PEAK | PML ( HIV) |
| 21 | LALAPPA M | 45 | M | HEADACHE, ALTERED SENSORIUM | Hyperintense | Hyperintense | _ | 190 | 9 | 190./97 | 9./97 | 97 | CHOLINE PEAK, LIPID LACTATE PEAK | TOXOPLASMOSIS |

| | | | | | | | | | | | | | |
|---|---|---|---|---|---|---|---|---|---|---|---|---|---|
| 22 | MAHADEVI TAKEKAR | 46 | F | HEADACHE, VOMITING, ATAXIA | Isointense | Hyperintense | + | 160 | 8 | 160./100 | 8./100 | 100 | RAISED NAA | TUBERCULOMA |
| 23 | MALLIKARJUN HIREMATH | 61 | M | HEADACHE, FEVER, MOTOR WEAKNESS | Isointense | Hyperintense | + | 190 | 9 | 190./103 | 9./103 | 103 | LIPID LACTATE PEAK, ICREASED TRE | MUCORMYCOSIS FUNGAL ABSCESS |
| 24 | MANJULA RACHGANI | 26 | F | HEADACHE, VOMITTING | Hypointense | Hyperintense | _ | 170 | 9 | 170./102 | 9./102 | 102 | RASSED CHOLINE, RAISED NAA | NCC |
| 25 | MANOHAR | 52 | M | HEADACHE, VOMITTING | Isointense | Hyperintense | + | 150 | 6 | 150./112 | 6./112 | 112 | LIPID LACTATE PEAK | TUBERCULOMA |
| 26 | MONICA | 30 | F | VOMITING, GIDDINESS | Isointense | Hyperintense | + | 190 | 9 | 190./100 | 9./100 | 100 | NORMAL | HSV ENCEPHALITIS |
| 27 | SUDHA PATANGE | 52 | F | VOMITING, HEADACHE | Hypointense | Hyperintense | + | 190 | 8 | 190./98 | 8./98 | 98 | LIPID LACTATE PEAK | |
| 28 | SHEETAL RAMAOGDE | 26 | F | HEADACHE ALTERED SENSORIUM | Hyperintense | Hyperintense | + | 170 | 9 | 170./99 | 9./99 | 99 | LIPID LACTATE PEAK | TUBERCULOMA |
| 29 | BALAPPA SANADI | 60 | M | SEIZURES,ALTERED SEBSORIUM | Hypointense | Hyperintense | + | 690 | 9 | 690./97 | 9./97 | 97 | CHOLINE PEAK | METASTASIS ( CA PROSTATE) |
| 30 | REKHA KELAGADE | 35 | F | HEADACHE, VOMITTING | Isointense | Isointense | + | 890 | 36 | 890./101 | 36./101 | 101 | NAA PEAK | GLIOMA |
| 31 | VIJAYLAXMI HANDRAL | 38 | F | HEADACHE, SEIZURES | Hypointense | Hyperintense | _ | 170 | 8 | 170./112 | 8./112 | 112 | RAISED NAA | NCC |
| 32 | SANGEETA KAMDOLI | 23 | F | HEADACHE, VOMITTING | Isointense | Hyperintense | _ | 107 | 7 | 107./102 | 7./102 | 102 | LIPID LACTATE PEAK | TUBERCULOMA |
| 33 | MAHAVEER MIRAL | 61 | M | ALTERED SENSORIUM | Hyperintense | Hyperintense | + | 870 | 34 | 870./100 | 34./100 | 100 | NAA PEAK | HIGH GRADE GLIOMA |
| 34 | MANISHA HANMANTACHE | 42 | F | SEIZURES, HEADACHE | Hypointense | Hyperintense | + | 802 | 35 | 802./111 | 35./111 | 111 | NAA PEAK | HIGH GRADE GLIOMA |
| 35 | CHANNAVA PATANSHETTI | 36 | F | HEADACHE, VOMITTING | Isointense | Hyperintense | - | | | | | | | |